

**COUNTING NUMBER OF POINTS FOR ACNE VULGARIS
USING UV FLUORESCENCE AND IMAGE PROCESSING**

MANITA KHONGSUWAN

**A THESIS SUBMITTED IN PARTIAL FULFILLMENT
OF THE REQUIREMENTS FOR
THE DEGREE OF MASTER OF SCIENCE
(TECHNOLOGY OF INFORMATION SYSTEM MANAGEMENT)
FACULTY OF GRADUATE STUDIES
MAHIDOL UNIVERSITY
2013**

COPYRIGHT OF MAHIDOL UNIVERSITY

Thesis
entitled
**COUNTING NUMBER OF POINTS FOR ACNE VULGARIS
USING UV FLUORESCENCE AND IMAGE PROCESSING**

.....
Ms. Manita Khongsuwan
Candidate

.....
Asst. Prof. Adisorn Leelasantitham,
Ph.D. (Electrical Engineering)
Major advisor

.....
Lect. Supaporn Kiattisin,
Ph.D. (Electrical and Computer
Engineering)
Co-advisor

.....
Lect. Waranyu Wongseree,
Ph.D. (Electrical Engineering)
Co-advisor

.....
Prof. Banchong Mahaisavariya,
M.D., Dip Thai Board of Orthopedics
Dean
Faculty of Graduate Studies
Mahidol University

.....
Lect. Supaporn Kiattisin,
Ph.D.
(Electrical and Computer Engineering)
Program Director
Master of Science Program in
Technology of Information System
Management
Faculty of Engineering,
Mahidol University

Thesis
entitled
**COUNTING NUMBER OF POINTS FOR ACNE VULGARIS
USING UV FLUORESCENCE AND IMAGE PROCESSING**

was submitted to the Faculty of Graduate Studies, Mahidol University
for the degree of Master of Science
(Technology of Information System Management)
on
April 10, 2013

.....
Ms. Manita Khongsuwan
Candidate

.....
Asst.Prof.Bunlur Emaruechi,
Ph.D.
(Environment Systems Engineering)
Chair

.....
Lect. Supaporn Kiattisin,
Ph.D. (Electrical and Computer
Engineering)
Member

.....
Asst. Prof. Adisorn Leelasantitham,
Ph.D. (Electrical Engineering)
Member

.....
Lect.Waranyu Wongseree,
Ph.D. (Electrical Engineering)
Member

.....
Asst.Prof.Werapon Chiracharit,
Ph.D. (Electrical and Computer
Engineering)
Member

.....
Prof. Banchong Mahaisavariya,
M.D., Dip Thai Board of Orthopedics
Dean
Faculty of Graduate Studies
Mahidol University

.....
Lect. Worawit Israngkul,
M.S. (Technical Management)
Dean
Faculty of Engineering
Mahidol University

ACKNOWLEDGEMENTS

The success of this thesis was attributed to attentive support from my major advisor, Asst. Prof. Adisorn Leelasantitham, my co-advisor, Lect. Supaporn Kiattisin, and Lect. Wanranyu Wongseree. I would like to express my sincere gratitude for all their invaluable encouragement, guidance, supervision and suggestion throughout this research.

I would like to say thank you to M.D. Waliorn Prachyapeang (Specialist of Dermatology) and M.T. Arporn Bureethan (Medical Technologist) from Institute of Dermatology in the case study, whom were involved in this Propionibacterium Acne (P.Acne) Laboratory project for providing information and suggestion.

A special acknowledgement goes to all the lecturers and staff of the Technology of Information System Management Program, Faculty of Engineering, Mahidol University for their services and support. I would like to thank all of my friends for their helps and encouragements.

Finally, thank you to the most important persons, my family members. I am very grateful for their entire support, care and their love throughout my whole life. They have inspired me to fight and overcome all obstacles, and allowed me to complete this research.

COUNTING NUMBER OF POINTS FOR ACNE VULGARIS USING UV FLUORESCENCE AND IMAGE PROCESSING

MANITA KHONGSUWAN 5437841 EGTI/M

M.Sc. (TECHNOLOGY OF INFORMATION SYSTEM MANAGEMENT)

THESIS ADVISORY COMMITTEE: ADISORN LEELASANTITHAM, Ph.D.,
SUPAPORN KAITTISIN, Ph.D., WARANYU WONGSEREE, Ph.D.

ABSTRACT

This research presents a method for counting the number of points for acne vulgaris using UV Fluorescence and image processing. There are five steps in the process of image processing as follows: 1) Use color processing to represent components of each image into three values including red, green, and blue colors, then indicate a value of global threshold using Otsu's method. 2) Find the optimal threshold (Automatic threshold) of selected layers of color image as shown in the histogram-threshold level. 3) Enhance image by Power-Law Transformation to determine the relative levels of the gamma correction function for improving and adjusting the P.Acne image and reduce the noise within the images. Moreover, this process corresponds to the optimal threshold in step 2, for the purpose of analyzing and proving relevancy using regression equations. 4) Segment the image by using the extended maxima transform which allows a binary image to be used for finding the difference between every pixel in the connection 8-ways. Each pixel must be more than the optimal threshold of step 2. This would automatically help separate objects from the background. 5) Automate counting by assigning a number label and an object number, which helps to specify points and calculate total points of P.Acne image.

An experiment with 50 samples of P.Acne images found the enhancement correlations method between the optimal threshold and the low-input value of the imadjust function by proving the linear equation. Also, the experimental results have shown that the accuracy, sensitivity, and precision are approximately at 92.45%, 95.76% and 96.39%, respectively. This helps in decreasing time consumption in analyzing P.Acne image and increase the efficiency of the process.

KEY WORDS: ACNE VULGARIS/ P.ACNE/ IMAGE PROCESSING

การนับจำนวนจุดสิวด้วยแสงยูวีฟลูออเรสเซนซ์ และกระบวนการประมวลผลภาพ

COUNTING NUMBER OF POINTS FOR ACNE VULGARIS USING UV FLUORESCENCE AND IMAGE PROCESSING

มนิดา คงสุวรรณ 5437841 EGTI/M

วท.ม. (เทคโนโลยีการจัดการระบบสารสนเทศ)

คณะกรรมการที่ปรึกษาวิทยานิพนธ์: อติสร ลีลาสันติธรรม, Ph.D., สุภาภรณ์ เกียรติสิน, Ph.D., วรัญญ วงษ์เสรี, Ph.D.

บทคัดย่อ

ผลงานวิจัยเล่มนี้ได้นำเสนอการนับจำนวนจุดสิวด้วยแสง UV Fluorescence และกระบวนการประมวลผลภาพ ซึ่งเราได้นำเสนอกระบวนการประมวลผลภาพมี 5 ขั้นตอน ดังต่อไปนี้ 1) การแยกภาพสีออกเป็นสามสีได้แก่ ระบายสีแดง ระบายสีเขียว และระบายสีน้ำเงิน โดยแสดงค่า global thresholding ปรากฏใน histogram ซึ่งใช้วิธี Otsu's method ในการแยกภาพสี 2)การหาค่า threshold ที่สูงสุดในแต่ละระบายของภาพสี ซึ่งได้แสดง histogram ในการแสดงค่า threshold ที่อยู่ในระบายสีที่โปรแกรมเลือกไว้ 3)ปรับปรุงภาพให้มีความคมชัดเหมาะสมในการประมวลผลภาพ(Enhancement) โดยการใช้กฎ Power-Law Transformations เพื่อใช้ในการกำหนดมาตรฐานความสัมพันธ์ค่าระดับ gamma correction เพื่อปรับปรุงความคมชัดในภาพและช่วยลดสัญญาณรบกวนในภาพแบบอัตโนมัติ โดยวิธีการนี้ช่วยทำให้เกิดความสัมพันธ์ระหว่างค่า optimal threshold ซึ่งสามารถนำมาวิเคราะห์ความสัมพันธ์เหล่านี้โดยใช้สมการความถดถอยเชิงเส้น 4)การแยกวัตถุออกจากภาพพื้นหลังโดยใช้กระบวนการ extended H- maxima transform จะมีการนำภาพที่ผ่านการ enhancement มาใช้ในการคำนวณและหาความแตกต่างระหว่างจุด pixel ซึ่งในภาพจะมีการเปรียบเทียบจุด pixel ทั้ง 8 ทิศทาง ซึ่งช่วยในการแยกวัตถุออกจากภาพพื้นหลังแบบอัตโนมัติ ส่งผลดีในการนับจำนวนจุดสิวในภาพได้อย่างรวดเร็ว 5)การนับจำนวนจุดสิวแบบอัตโนมัติโดยสามารถระบุป้ายตัวเลขของแต่ละจุดและคำนวณค่าผลรวมของจุดสิวทั้งภาพ

ผลจากการทดลองจากภาพสิว 50 ภาพเป็นตัวอย่างทำให้เกิดความสัมพันธ์การปรับปรุงภาพระหว่างค่า optimal threshold และค่า low-input ในฟังก์ชัน imadjust โดยการพิสูจน์จากสมการเส้นตรง ซึ่งสามารถนำไปสรุปเป็นค่าความถูกต้อง ความไว และความแม่นยำ ประมาณ 92.45 %, 95.76% และ 96.39% ตามลำดับ ซึ่งผลการวิจัยนี้สามารถช่วยในการประหยัดเวลาด้านการนับจำนวนจุดสิวและช่วยในการวิเคราะห์ภาพสิวได้อย่างมีประสิทธิภาพ

CONTENTS

	Page
ACKNOWLEDGEMENTS	iii
ABSTRACT (ENGLISH)	iv
ABSTRACT (THAI)	v
LIST OF TABLES	viii
LIST OF FIGURES	ix
CHAPTER I INTRODUCTION	1
1.1 Background and statement of problems	1
1.2 Objective of study	5
1.3 Scope of work	5
1.4 Results	6
CHAPTER II LITERATURE REVIEW	7
2.1 Basic Knowledge of P.Acne	7
2.1.1 Fluorescence spectroscopy for endogenous porphyrins	
In human facial skin	10
2.2 Image Processing	10
2.2.1 Image Segmentation Using Multithresholding of	
Second-Order –Gray-Level Statistics	11
2.2.2 Grain Counting Method Based On Image Processing	12
2.2.3 Digital Image Analysis Based Automated Kiwifruit	
Counting Technique	13
2.2.4 Automatic Counting of Fission Tracks using	
Object-Based Image Analysis for Dating Applications	13
2.2.5 Counting Ear Rows in Maize Using Image Process	
Method	14
2.2.6 Automatic Counting of Leukocytes in Giemsa-Stained	
Images of Peripheral Blood Smear	14

CONTENTS (cont.)

	Page
2.2.7 Counting Method of Heterotrophic Bacteria Based on Image Processing	15
2.2.8 A New Method for Blood Cell Image Segmentation and Counting Based on PCNN and Autowave	16
2.2.9 Counting Moles Automatically From Back Image	16
2.2.10 Evaluation of spatial and temporal variability of the physical characteristics of berries olives (<i>Olea europaea</i> L.) Arbeqiana variety, using image technology processing	16
2.2.11 Automatic Embryonic Stem Cells Detection and Counting Method in Fluorescence Microscopy Images	17
2.3 A Power Law Transformation Predicting Lightness Conditions Based on Skin Color Space Detection	17
2.4 Regression Analysis: Basic Concept	19
CHAPTER III RESEARCH METHODOLOGY	22
3.1 Research methodology	22
3.1.1 Color Image Processing	23
3.1.2 Global Thresholding	25
3.1.3 Image Enhancement	27
3.1.4 Histograms	33
3.1.4.1 Histogram Stretching (Contrast Stretching)	34
3.1.5 Image Topology	37
3.1.5.1 Extended Maxima transform	37
3.1.5.2 Labeling	38
3.2 Verification of performances	40
CHAPTER IV RESULTS AND DISCUSSION	42
4.1 Verification of performances by image processing	44

CONTENTS (cont.)

	Page
4.2 Discussion of counting P.Acne points by image processing	47
CHAPTER V CONCLUSION AND RECOMMENDATION	51
5.1 Conclusion	51
5.2 Recommendation	51
5.2.1 Image processing technique improvement	51
REFERENCES	53
APPENDICES	55
Appendix A The relationship threshold using SPSS tool	56
Appendix B Flow chart of counting PAPs by image processing	60
Appendix C Comparing P.Acne between Manual and Auto mehtod	61
BIOGRAPHY	81

LIST OF TABLES

Table	Page
1.1 Skin problems evaluated using VISIA camera	3
2.1 Example of finding residuals	21
3.1 The descriptive statistic	30
3.2 The regression model summary	31
3.3 The Coefficients Model	31
3.4 The bivariate correlations table	33
3.5 The verification of the P.Acne	40
4.1 The results of counting number of the P.Acne points comparing between human eye and image processing	44
4.2 The overall results of performances in terms of three indicators i.e. accuracy, sensitivity and precision	46
4.3 The comparing counting method between manual processing and image processing	46
4.4 The value threshold of P.Acne image of 50 samples	49

LIST OF FIGURES

Figure	Page
2.1 UV Fluorescence images of the P.Acne	8
2.2 Face of a patient taken by the photo using VISIA camera based on the UV Fluorescence (UVF)	9
2.3 A process of manually counting the P.Acne image Using the human eye of technician in Institute of Dermatology	9
2.4 Image of skin showing the presence of porphyrins acquired From blue-excited fluorescence imaging	10
2.5 A graph shows relation between predicted brightness versus original brightness (energy)	18
2.6 A graph shows relation between light energy versus brightness at particular pixel.	18
2.7 Regression residual	20
3.1 A proposed method of automatically counting number of the P.Acne Points using the UV Fluorescence and image processing	23
3.2 A three dimensional array for an RGB image	24
3.3 An original color image of P.Acne	24
3.4 An RGB color image components of P.Acne	25
3.5 The gamma correction level by Power-Law Transformation	27
3.6 Improving contrast of the P.Acne image by gamma correction	28
3.7 Histogram of improving contrast of the P.Acne image by gamma correction	29
3.8 The linear regression between the optimal threshold and the Low input value of imadjust function of P.Acne points	30
3.9 Histogram of the original of P.Acne image	34

3.10	The stretching function given by imadjust	35
------	---	----

LIST OF FIGURES (cont.)

Figure		Page
3.11	The imadjust function with gamma not equal to 1	35
3.12	The P.Acne image before and after adjustment by imadjust function	36
3.13	The image and histogram resulted from Extended H-Maxima Transform	38
3.14	Results comparing between the manual and the automatic counting number of P.Acne points using labeling method	39
4.1	The chart diagram of three major methods of P.Acne counting by using image processing	42
4.2	Seven samples image: 12(1), 13(2), 18(3), 19(4), 25(5), 34(6) and 43(7) show missing the P.Acne points	47

CHAPTER I

INTRODUCTION

1.1 Background and Statement of Problems

The patients for treatments of Acne disease have been increasing annually. According to the Institute of Dermatology (INDERM), the Acne disease is ranked second inferior to eczema disease [1]. The INDERM receives 30,000 patients per year and 3,000 of them are suffering from Acne disease. It was reported that 90% of patients in Thailand did not seek doctors for treatment of Acne because they thought that Acne concerns their beauty. As a result, they use over the counter medicine or cosmetics to treat the Acne patients or consult with the beauticians in salons. In fact, the Acne disease is a dermatology which has been frequently found in Thailand [2]. Acne disease is caused by Androgen Hormone of male stimulating the function of fatty gland on the skin to build and release more having fatty acid. However, this could also be found in female. Female has an opportunity of Acne disease but less than male. When the fatty gland produces more fatty acid and the pore tube will produce cells of pore for combining the Acne called "comedone" in the tube of the fatty gland. Two types of the comedone are as follows. First type: the comedone is not an inflammation e.g. "white or closed comedone" and "black or open comedon". On one hand, if the tube of fatty gland does not exposed to the air, then the comedone would not touch be exposed to the air and it would be a white color of fatty point called "white or closed comedone". On the other hand, if the comedone opens the tube and is exposed to the air (or the oxygen in the air), then the color of the Acne would be change from dark to black color. This would be called "black or open comedone". Second type, the comedone is an inflammation e.g. red pimple and pus-filled pimple. This is caused by the bacteria called "Propionibacterium Acne (P.Acne)" which stays in the hole of the fatty gland. This type of bacteria does not use oxygen, but it would digest fatty acid as its food and produce fatty acid which causes irritation, pus, and

inflammation. Therefore, the treatment method would differ between the two types [3].

In addition, VISIA camera would allow us to obtain 3 types of images. First, Image taken under normal light; the image would be similar to those taken by typical cameras providing normal colors. Second, image taken under Cross Polarized; the reflection from the skin would be eliminated. Therefore, the image would contain only the reflection from the layer under the skin. This would be for the purpose of finding the melanin and hemoglobin e.g. blemish, freckle and redness from Acne. Third, Image taken under UV Fluorescence; the image would be taken during the emission of the wavelength range of 364 nm where the light would be absorbed by the pigment of melanin under the skin. Therefore, the abnormality of the skin color would be shown e.g. blemish and freckle. Moreover, in this method is Porphyrin which indicates the probability of Acne vulgaris occurrence. It is clear that the 3 types of images that could be obtained using the VISIA camera would help in evaluating different skin types and conditions as the images would help to see the problems underneath the skin which could not be seen with the naked eyes. Other than the in-depth analysis which the VISIA camera provides, the benefits of using the VISIA camera are as follows:

- The benefit in term of treatment. After using and evaluating the images taken, we could analyze the basic skin problem specifically for the particular patient and decide the treatment that best fits that particular patient.
- The benefit in prevention. Certain conditions cannot be seen by the naked eyes, but could be detected by the VISIA camera such as the detection of P.Acne, freckles underneath the outer skin layer. Therefore, the treatment plan could be designed to prevent P.Acne and freckles from appearing on the outer skin layer that could be seen by the naked eyes.
- The benefit in follow-up a treatment. We could evaluate the treatment by comparing the image taken before treatment and image taken after treatment. This would help in clarifying incremental changes that occur during the treatment. VISIA camera would help in analyzing problems including Acne scars, blemish, freckle and nearly all skin wrinkle problems on the face. Furthermore, the usage of the device that could help analyze in detail would help improve the analysis of skin problem and help

planning the treatment to target that specific problem. This would lead to creating an effective treatment.

Evaluating the skin problem with VISIA camera would help analyze to the level of skin cells in Table 1.1.

Table 1.1 Skin problems evaluated using VISIA camera

Skin Problems	Skin Analyzing Technique
Spots e.g. freckles, hyper-pigmentation from Acne, capillary redness	Measuring the difference in colors of the disease marks with the background of the skin color.
Pores	Measuring the shadows of the pores that are darker than the normal skin areas would indicate the locations of larger pores.
Wrinkles	Measuring the difference in skin's height surface by using the difference in color levels.
Porphyrin	Measuring the fluorescence area to find the quantity of P.Acne and the possibility of Acne Vulgaris caused by a bacteria as Porphyrin is a fluorescent substance which would absorb and emit light under the UV Fluorescence
UV Spots or Abnormality of skin pigment caused by UV light e.g. blemish	Measuring the areas clearly seen as the light would be absorbed by the melanin pigment and make the abnormality caused by melanin pigment in the skin layer of epidermis becomes distinct.
Red area and brown spots e.g. black or red birthmarks	Measure the intensity and size of the area that is dark by using the RBXtm technology.

Therefore, from the qualities stated above, counting of P.Acne could be performed by using the theory of fluorescence by counting the glow spots within the image without having to consider the skin condition or the fat density underneath the skin.

From the information stated above, specialist of medical dermatology performs research and cooperates with the medical technician of the bioengineering unit of Dermatology, which includes planning and testing the growing rate of the P.Acne. In the experiment, the number of the Acne points is counted by human eye from an image based on the VISIA camera i.e. a photo of UV Fluorescence that helps to see the image more clearly. However, there are many problems for counting such the number of acnes as the result could be inaccurate due to human flaws, together with the fact that the Acne image is difficult to see, analyst and distinguish the Acne points. Also, the human eye cannot see the image clearly depending on patients' surface of skin. As a result; they may analyze the image incorrectly. Counting number of organism is important as it is a fundamental stage leading to the analysis and would then be for various applications. Counting number of organisms could be divided into 4 groups: (1) cell group: blood cell and leukocyte [4-5]; (2) plant group: pollen grain, grain and kiwifruit [6-8]; (3) animal group: fish and Peruvian scallop larvae [9-10]; (4) bacteria group: heterotopic, colony, spores [11-13]. However, the related researches have not presented the count of number of the P.Acne points (PAPs) using image processing because they could not be seen by human eyes. Therefore; it will use the counting technique to preview the Acne image taken by the photo of the UV Fluorescence. This Acne is reflected with the UV Fluorescence and it is a small point which is a type of bacteria.

In this research, counting number of points for the P.Acne vulgaris is presented through the use of UV Fluorescence and image processing. Currently, the Institute of Dermatology still uses human eyes in counting numbers of the PAPs from an image of the UV Fluorescence. This method uses a process of image processing this includes. Cropping a UV image and selected a region of interest, then the cropped image (or the color image) is then used for a color processing to represent components of each image as three values including red, green, and blue color showing a value of global thresholding using Otsu's method. After that, find the optimal threshold (Automatic threshold) of selected layers of the color as shown in the histogram-threshold level. In addition, we have to make image adjustment by using Power-Law Transformation to determine the relative levels of gamma correction function in order to improve and adjust the P.Acne image and reduce noise within the images.

Moreover, this process is related the optimal threshold for the purpose of analyzing and proving relevancy using regression equations. Next step is the image segmentation, by using the extended-maxima transform which allows binary image to be used for finding the difference between every pixel in a connection 8-ways and each pixel must be more than optimal threshold. This process sets to the H-maxima transform into a white color point called “object”, but if it is less than the level set to the H-maxima transform into a black color point called “background”. This helps to separate objects from the background automatically. Finally, counting the P.Acne point automatically by assigning number label and objects number, which help to specify points and calculate total points of all P.Acne of the image.

From the experimental results of 50 images, the accuracy is more than 90% and it saves time to analyze the P.Acne points. The advantage of this method enables its user with accurate information the Acne points count for the purpose of recording statistic reports and enable comparison between before and after a treatment of Acne patients.

1.2 Objective of Study

- 1) To improve the manual counting method of the P.Acne point by image processing.
- 2) To enhance the Acne patient's image using UV Florescence by effective image processing.
- 3) To decrease time of counting the P.Acne points comparing to the current from manual counting process.

1.3 Scope of Work

This research consists of improving the Acne patient's image from information of Bioengineering LAB in Institute of Dermatology. Its details are as follows:

- 1) Taking photo of patient's face by using the UV Fluorescent light with VISIA camera (Special camera for Bioengineering LAB).
- 2) Using images of 50 samples of acne patients.
- 3) Cropping each of the Acne patient image to size 1 cm² or image size equals to 118X118 mm (width x length).
- 4) Identify features of P.Acne points in the Acne patient's image from reflex UV Fluorescent light called "Porphyrin".
- 5) Counting total number of P.Acne points in the Acne patient's image.
- 6) Concluding and recording number of the P.Acne points for the doctor to analyze respectively.

1.4 Results

Image processing has modified the manual counting method of P.Acne point. It is suitable for specifying the P.Acne points as it is fast and efficiently with the following points:

- 1) To decrease mistake on counting the P.Acne points from the Acne patient's image using UV Fluorescent light.
- 2) To improve the manual counting method by making it easier.
- 3) To specify interested object more clearly.
- 4) To save time of counting P.Acne points and analyzing.
- 5) To reduce task of medical technician.

CHAPTER II

LITERATURE REVIEW

This research reviews basic knowledge of P.Acne and image processing for improvement of manual counting method via the P.Acne's patient image using UV Fluorescence from Bioengineering LAB in Institute of Dermatology. Therefore, the image processing shows that the P.Acne points around the nose area of skin surface after taking photo of the Acne patient using the UV Fluorescence light. In addition, this thesis includes advantages and disadvantages comparison between manual process and automatic process, which relates to the analysis from the accuracy value of the experiment and using regression analysis model to prove relations between the threshold value and the gamma correction value by "Power Law Transformation". Also, this enhanced the image to become a higher quality image and reduce the noise within the images. In addition, usage of extended H-maxima transform was employed for separating object and background that helps in counting the number of P.Acne points more efficiently.

2.1 Basic knowledge of P.Acne

The Acne can be classified into several skin lesions including comedo, reddish papule, papule, pustule, and scar that are difficult for the proper evolution of Acne skin lesion and that are infected in orthopedic implants associated with the Acne vulgaris [14]. P.Acne is a gram positive anaerobic microorganism where the major skin bacterium causes the Acne. The dynamic of inflammatory Acne, consisting of immunologic factors with the P.Acne, is triglyceride fraction of sebum. It is the dominant organism in sebaceous follicles and the P.Acne antibodies whose alternative pathway is mediated by carbohydrates derived from cell walls of the bacteria. In addition, the P.Acne produces Porphyrin which fluorescence under Wood's light, appearing on the nose, a close-up image on surface, as shown in Figure 2.1 (a) and

Figure 2.1(b). The Acne also produces Porphyrin which absorb light energy of the near ultraviolet (UV) and blue light energy [15].

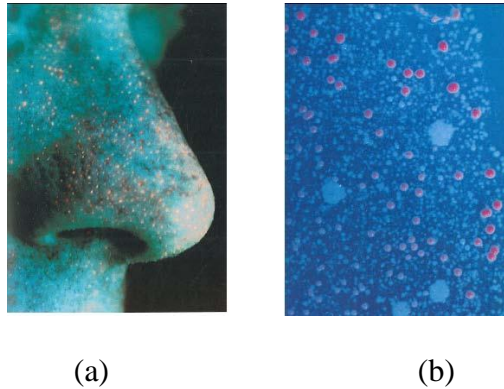


Figure 2.1 UV Fluorescence images of the P.Acne

(a) Wood's light appearing at the nose and (b) Close-up image on surface.

Figure 2.2 shows a face of the patient which is taken by the photo using the VISIA camera based on the UV Fluorescence (UVF). Figure 2.3 shows a process of technician manually counting the P.Acne image using human eyes in Institute of Dermatology. It can be seen from Figure 2.2 that a medical technician takes the photo of an Acne patients to capture Acne image using VISIA camera based on the UV Fluorescence light. The P.Acne points affects the UVF light and it is appears in the orange light, but sometimes this point is unclear. The technician could enlarge the Acne image, even though it would become blurry, but it enables him to see the Acne point. Next, the technician crops a region of interest on the nose surface; from the image sized approximately 1 cm^2 , as this area consists of the P.Acne points more than other region. And then, the technician used a program of marking tool which helps to count the P.Acne points from the cropped image. This process used more time to count and analyze, since the human eye cannot see every points of the cropped image that is not clear therefore, effects difficulty of counting the Acne points. Also, some surface could be miscounted. Finally, the result of counting number of the P.Acne points is recorded in a report which would further be analyzed and diagnosed from a medical doctor. The doctor would analyze the growing rate whether increasing or decreasing

within the duration a comparison between before and after the Acne treatment. The treatment will help to prevent the Acne patient from having future Acne vulgaris.

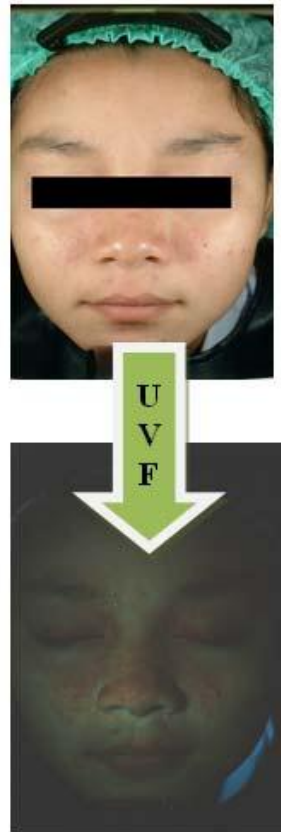


Figure 2.2 Face of a patient taken by the photo using VISIA camera based on the UV Fluorescence (UVF).

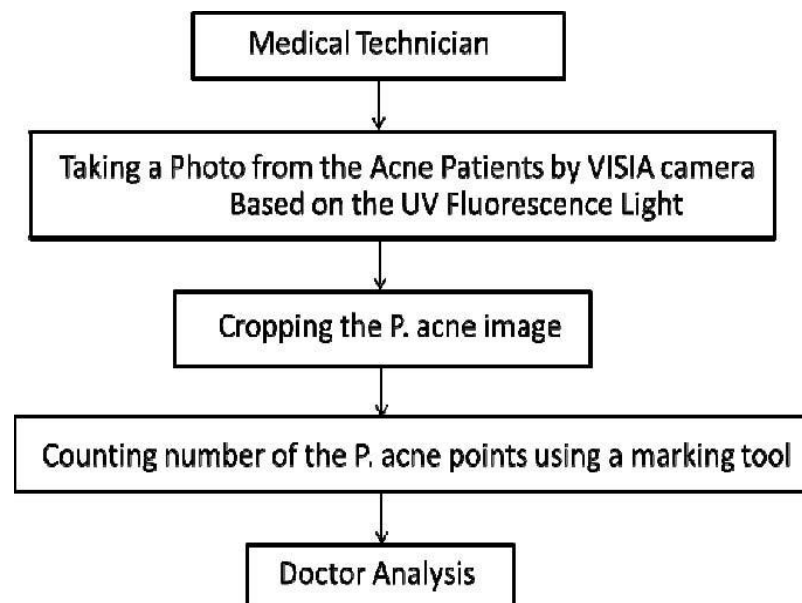


Figure 2.3 A process of manually counting the P.Acne image using the human eye of technician in Institute of Dermatology

2.1.1 Fluorescence spectroscopy for endogenous Porphyrin in human facial skin

This research proposed the overview of the development of Acne vulgaris due to the presence of porphyrin-producing *Propionibacterium Acnes* (*P.Acnes*) inside sebaceous follicles of human facial skin [16]. The bacteria are known to produce coproporphyrin, a tetrapyrrole molecule, as a result of its metabolism. Coproporphyrin can be excited with blue light to produce fluorescence in the red region of light spectrum. Fluorescence imaging excited by blue light has been extensively used to disclose the presence of Coproporphyrin and the activity of *P.Acnes* as shown in Figure 2.4. Also, our research can prove the objects by using UV Fluorescence light that help to specify the characteristic of *P.Acne* point more clearly.



Figure 2.4 Image of skin showing the presence of Porphyrin acquired from blue-excited fluorescence imaging

2.2 Image Processing

Image Processing involves how to improve the original digital image to become more suitable for human interpretation and autonomous machine perception [17]. Therefore, if we have still image information, image processing would be a tool to help analyzing and solve problem from original image and improve image data to increase efficiency.

This research reviewed and studied about the subject method and applied with our research, which is related to improving the process of manually counting with

the use of image processing, such as the color processing and classifying the threshold value from the color image using Otsu's method. This is find the optimal of threshold for making automatic threshold, adjustment of image by using Power-Law Transformation for building the model of relative the optimal threshold value and the Low-input value of imadjust function, then proving the relevancy using regression equation. Image segmentation between the objects and background by H-maxima transform function and further count the total numbers of points automatically, as follows;

2.2.1 Image Segmentation Using Multi-thresholding of Second-Order –Gray-Level Statistics

This research proposed the overview of automatic threshold selection method using the gray image [18]. It used co-occurrence matrix until histogram brought data to calculate for finding multi-thresholding by using Otsu's algorithm. This process helps segmentation of image to become better by using the image histogram. Also, we are applying the Otsu's algorithm for finding automatic threshold of the color image as follows.

In Otsu's method, we can search for the threshold that minimizes the intra-class variance (the variance within the class), defined as a weighted sum of variances of the two classes in equations at (1):

$$\sigma_{b(t)}^2 = \omega_1(t)\sigma_1^2(t) + \omega_2(t)\sigma_2^2(t) \quad (1)$$

Weights ω_i are the probabilities of the two classes separated by a threshold t and σ_i^2 variances of these classes. Otsu shows that minimizing the intra-class variance is the same as maximizing inter-class variance in equations at (2):

$$\sigma_{b(t)}^2 = \sigma^2 - \sigma_{\omega}^2(t) = \omega_1(t)\omega_2(t) [\mu_1(t) - \mu_2(t)]^2 \quad (2)$$

Which is expressed in terms of class probabilities ω_i and class means $\mu(i)$. The class probability $\omega_1(t)$ is computed from the histogram as t in equations at (3):

$$\omega_1(t) = \sum_0^t p(i) \quad (3)$$

While the class mean $\mu_1(t)$ in equations at (4) as follows:

$$\mu_1(t) = \sum_0^t p(i)\chi(i) \quad (4)$$

Where $\chi(i)$ is the value at the center of the histogram binary. Similarly, we can compute $\omega_2(t)$ and μ_t on the right-hand side of the histogram for bins greater than t . The class probabilities and class means can be computed iteratively. This idea yields an effective algorithm.

Otsu's Algorithm

- Compute histogram and probabilities of each intensity level
- Set up initial $\omega_i(0)$ and $\mu_i(0)$
- Step through all possible thresholds $t = 1$ (maximum intensity)
- Update the value of ω_i and μ_i
- Compute $\sigma_b^2(t)$
- Desired threshold corresponds to the maximum $\sigma_b^2(t)$
- We can compute two maxima (and two corresponding thresholds). $\sigma_{b1}^2(t)$ is the greater max and $\sigma_{b2}^2(t)$ is the greater or equal maximum
- Desired threshold = $\frac{\text{threshold}_1 + \text{threshold}_2}{2}$

2.2.2 Grain Counting Method Based On Image Processing

This paper presented improves grain counting method by image process that can effectively resolves the overlaps and conglomerations among grains by mechanical vibration and image erosion processing [7]. This process is transforming color image to gray image and using image de-noising for reduce noise out of the original image. In addition, this paper shows the best threshold from image by function graythresh that automatically analyzes grayscale histogram and determines the optimal threshold according to the histogram and using image erosion processing

to eliminate boundary point suitable for counting the number of grains. Moreover, we could obtain any process to apply with our new process to reduce noise within the original image and find value thresholding in each image for classification of P.Acne point continuous.

2.2.3 Digital Image Analysis Based on Automated Kiwifruit Counting Technique

This paper used the digital image analysis techniques for developing an automated kiwifruit counting system [8]. The methods containing minimum distance classifier based segmentation technique in L^*a^*b color space for data extraction and Analysis two kiwifruit varieties namely Gold and Green.

This paper mainly focuses on classification. Classifying each pixel into its region to eliminate noise by morphological open operation and achieve automatic counting, the images converted into gray color image for evaluation, kiwifruit counted from the segmented images with three methods such as Regional Maximum (RM), Distance Transform (DT), and Area. From this paper, pre-processing, color segmentation and counting number of kiwifruit on the image interested were shown. The methods color of segmentation and automated counting could be applied in our research because the P.Acne points in UV Fluorescence image have two color points on the facial skin and objects could then be extracted out of the background for automated counting.

2.2.4 Automatic Counting of Fission Tracks using Object-Based Image Analysis for Dating Applications

This paper presented Geochronological dating with the fission-track method is time consuming and induced tracks [19]. Also, Image analysis base on the microscopic images to difficult classify objects. Therefore, it is developed the original image to the digital images in pre-processing for ensure a proper segmentation and reduce the heterogeneity and used non-linear transformation for identify image. Next, this paper is used optimum feature identification for calculation based on SEaTH that delivers with the highest separabilities between track and background. In the sample, this acts as input for the intermediate clustering and classification after finding the thresholds for the most suitable features and a manual refinement and counted by

processing the skeletons. Also, this helps on clustering and classification of P.Acne regarding circumspect and finding the thresholds for most suitable with P.Acne point.

2.2.5 Counting Ear Rows in Maize Using Image Process Method

This paper presented Ear Rows, an important agricultural character in Maize using new counting process based on edge marker and discrete curvature [20]. In procedure, image obtained by scanning images and using image processing to find characteristic of shape, color, texture of the corn seed. In this paper, relationship between shape and parameter is clearly determined for analyzing variety of character and using median filter to fill the inner holes and remove the internal interference with a dark circle. Then the edge could be found and figure out the distribution of the function of the edge radius r with the method of edge marking. Therefore, this paper inspires the idea of constructing the counting model and improving the edge of image by using image processing to enhance efficiency.

2.2.6 Automatic Counting of Leukocytes in Giemsa-Stained Images of Peripheral Blood Smear

This paper presented a variety of classes of leukocyte in peripheral blood image using image segmentation for semi-automatic to segment cell and automatic counting of the interested cell [5]. These method include thresholding, watershed, nearest neighborhood graphs, mean shift procedure and deformable model, which divided into three major categories: Boundary based, Region based and Thresholding is applied to some extracted image feature by Otsu and Wu for choosing a suitable threshold and calculating the image variance to separate the cell from the background. In addition, this paper used histogram analysis where maximum amount in histogram is related to intensity of background pixel of image and selection of appropriate point for thresholding of red cells pixel in the image. Consequently, a point with less intensity than local maximum is the suitable point and using basic morphological operation are dilation; add pixels to the boundaries of objects in an image, while erosion removes pixels on object boundaries. Then number from binary image could be counted and set pixel dilation is to the value 1 by automatically. Also, our research used thresholding method to apply a histogram image for analyzing and specifying the capability between P.Acne thresholding and Background thresholding.

2.2.7 Counting Method of Heterotrophic Bacteria Based on Image Processing

This paper presented Heterotrophic detected and counted by image processing [11]. These methods include thresholding with grayscale-weighted, distance transform and applied watershed algorithm to segment overlapping colonies. Finally four-connect searching algorithm was used to mark and count the colony. Therefore, this paper is made binarization of colony image to consider the method threshold segmentation and separated the colonies from background by setting color for background equals 1 and colonies equals 0 for classification purpose. In addition, there are two methods of thresholding for segmentation image. First method is the iteration threshold method is finding minimum and maximal intensity value in original threshold (5) for proceeding of counting. Second method is the grayscale-weighted threshold method is basically similar to the first one but it obtain a threshold through finite iteration for difference between original threshold value (6) and new threshold value (7) and determine segmenting threshold by choosing different threshold weight coefficients according to specify case of the image.

$$T0 = (Z_{min} + Z_{max}) / 2 \quad (5)$$

$$T0 = \omega Z_{min} + (1 - \omega) Z_{max} \quad (6)$$

$$TK + 1 = \omega Z0 + (1 - \omega) ZB \quad (7)$$

From this paper, we can obtain the Iteration threshold method to support our research because this method is a step to select the max threshold value from region color image of the P.Acne image by using UV Fluorescence.

2.2.8 A New Method for Blood Cell Image Segmentation and Counting Based on PCNN and Autowave

This paper proposed the Autowave characteristic of PCNN for blood cell image segmentation and counting [4]. The paper includes 3 methods as follows: First, the image is de-noised using PCNN model combined with median filter. Then in order to segment blood cells from its background based on minimum cross-entropy. Finally, autowave is carried out to eliminate small disturbed objects (noncell objects) in the cell image. At the same time the cell's number can be counted and a specific cell can be segmented from its background through labeling each blood cell. This

process used complexity of cell that is impossible for us to get a uniform method to segment any other types of image, but this paper presented new technique of PCNN Model combined with median filter which is an essential knowledge for image processing.

2.2.9 Counting Moles Automatically From Back Image

This paper proposed density of moles, a strong predictor of malignant melanoma by automatic method of segmenting and counting moles compared with manual counting [21]. Three methods mentioned in this paper are as follows: finding the moles, selection of candidate moles, and use of feature space to identify true moles. In the finding of moles each candidate is classified as moles or not, such as removal of noise using the mean shift algorithm for good clustering algorithm that preserves each cluster. Also, comparison of new algorithm with a simple finding mole is more accurate. Then our research can apply the findings of different contrast threshold value to improve the threshold of regions image and compare between manual process and image process making this more efficient.

2.2.10 Evaluation of spatial and temporal variability of the physical characteristics of berries olives (*Olea europaea* L.) Arbeqiana variety, using image technology processing

This paper proposed a model that captures photographs of branches with fruit, on specific points within a block, determined by aerial images [22]. Process images using cross-correlations with Eigen-image data set perform with and neural networks to discern on the fruit in the picture. The results compared in field measurements with precision instruments, generated estimate of physical variables close to the proposed error (0.3 mm), with R^2 of 0.64 relations. Also, our research have applied the statistical inference for the analysis of color image data and this helps in building model of relationship between the threshold value and the low input value of imadjust function for the purpose of successive automatic run in the program.

2.2.11 Automatic Embryonic Stem Cells Detection and Counting Method in Fluorescence Microscopy Images

The paper focuses on automatic embryonic stem cell detection and counting method for fluorescence microscopy images [23]. The proposed method is interesting characteristic such as the pixel of a cell are lighter in the middle and the pixel's luminance value decreases gradually as it reaches the cell boundaries. Pre-processing used Gaussian filter with radius to reduce the noise and emphasize the local maximum points that separate the cell from the background using a threshold, histogram partition, and connected component detection. The output of this step is a matrix M with the same dimensions of the input image. In addition, this paper includes the construct of a region-adjacency graph $G = (V, E)$ based on M and in the graph G , each stem cell is represented by a sub graph S that is S contains more than one node for finding the simple path pattern and solution for automatic counting. Moreover, this paper is exclusively for appropriated microscopy image, micro object where the error exist if two or more cells are positioned near to one another would be seen as one light point. Also, our research applied the image characterization from object in UV Florescence image where classification of data is satisfied.

2.3 A Power Law Transformation Predicting Lightness Conditions Based on Skin Color Space Detection

This paper presents an improved human-skin-color detection approach in images using power law transformation predicting lightness conditions [24]. The approach of this paper was focused on different illumination conditions and complex background via RGB-HSV model. The illumination is adjusted without losing image's quality, and skin detection is done in a per pixel fashion after transforming into HSV color space. The experimental results demonstrated that, the proposed technique is able to achieve robust results, where a set of skin color images from ethnic color images of ethnic groups have been detected such as Asian, African and Caucasian.

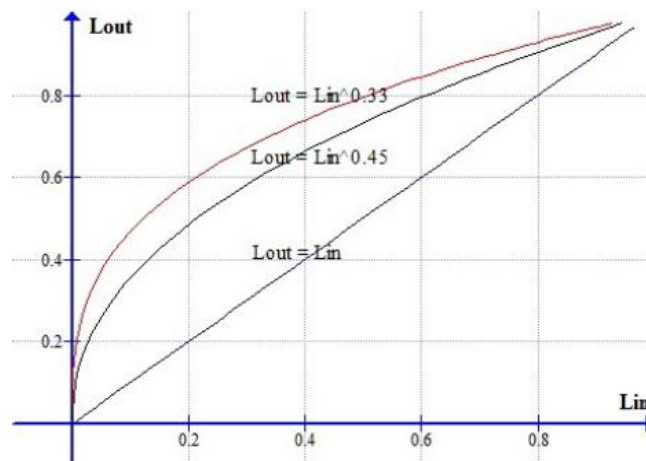


Figure 2.5 A graph shows relation between predicted brightness versus original brightness (energy).

In the paper method, enhancement of images by robust skin color detection and convert an image into specified color space, segments each pixel to either a skin or non-skin and refines spatial homogeneity on each detected, such as closing and opening techniques. In the Figure 2.5, a power law transformation has been computed to predict lightness due to illumination differences. Then the result of enhance lighting compensation for various values of gamma p different levels of enhancements can be obtained for gray scale image also can be easily applied for further contrast and high lighting in the Figure 2.6.

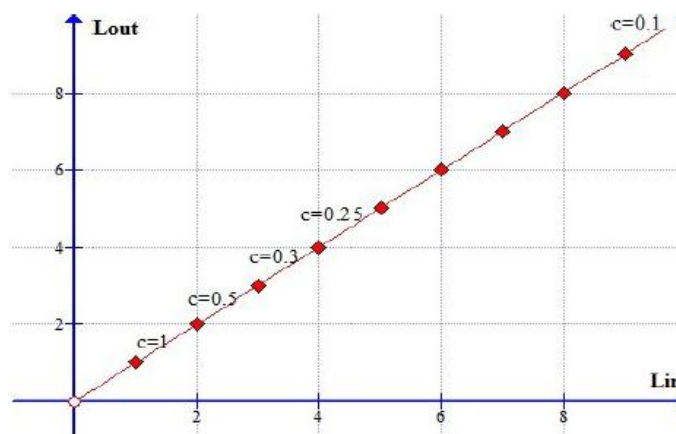


Figure 2.6 A graph shows relation between light energy versus brightness at particular pixel.

From this paper, our research applied the power law transformation to create a relationship between the optimal thresholding value and the low-input value of imadjust function for improving image to be more distinct and adjust the contrast light in the UVF image experiment's efficiency.

2.4 Regression Analysis: Basic Concept

This paper presented the simple linear model and goodness of fit for applies technique with variable of interest [25] such as y is dependent variable and x is independent variable. The simple linear equation (8) is as follows:

$$y_i = \beta_0 + \beta_1 x_i + u_i \quad (8)$$

This equation parameter represents the y-intercept and slope of the relationship, respectively. In this model, it makes some assumptions about the behavior of the error term in three things:

- $E(u_i) = 0$ u has a mean of zero for all i
- $E(u_i^2) = \sigma_u^2$ it has the same variance for all i
- $E(u_i u_j) = 0, i \neq j$ no correlation across observations

We define the estimated error or residual associated with each pair of data values as the actual y_i value minus the prediction (9), based on x_i along with the estimated coefficients as following:

$$\hat{u}_i = y_i - \hat{y}_i = y_i - (\hat{\beta}_0 + \hat{\beta}_1 x_i) \quad (9)$$

In a scatter diagram of y against x, this is the vertical distance between observed y_i and the fitted value, \hat{y}_i , as shown in Figure 2.7.

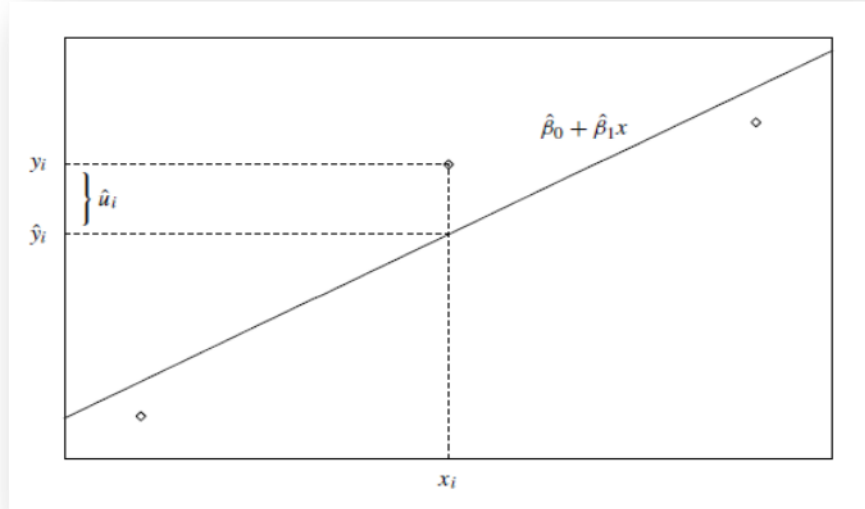


Figure 2.7 Regression residual

In goodness of fit, the OLS technique that finds the values of β_0 and β_1 fit the sample data best in the specific sense of minimizing the sum of squared residuals. Then subtract each fitted value from the corresponding actual, observed, value of y^i in Table 2.2. As shown, the magnitude of the SSR depends on the number of data points in the sample. The square root of the expressed result is called the estimated standard error of the regression (10) in this equation:

$$\hat{\sigma} = \sqrt{\frac{SSR}{n-2}} \quad (10)$$

A more standardized statistic, which also gives a measure of the goodness of fit of the estimated equation (11), it is R^2 . This statistic is calculated as follows:

$$R^2 = 1 - \frac{SSR}{\sum (y_i - \bar{y})^2} = 1 - \frac{SSR}{SST} \quad (11)$$

Also, R^2 can be written as 1 minus the proportion of the variation in y_i that is explained by the estimated equation. As such (12), it must be bounded by 0 and 1.

$$0 \leq R^2 \leq 1 \quad (12)$$

$R^2 = 1$ is a perfect score, obtained only if the data points happen to lie exactly along a straight line; $R^2 = 0$ perfectly lousy score, indicating that x_i is absolutely useless as a predictor for y_i . In order to judge, whether it is the best-fitting line or not an adequate degree of data is required.

Therefore, our research obtained the regression analysis to summaries the tendency of data sample in the experiment and it helps proving the assumption about the relationship between the optimal thresholding value and the low-input value of imadjust function.

Table 2.2 Example of residuals finding

Given $\hat{\beta}_0 = 52.3509$; $\hat{\beta}_1 = 0.1388$				
data (x_i)	data (y_i)	fitted (\hat{y}_i)	$\hat{u}_i = y_i - \hat{y}_i$	\hat{u}_i^2
1065	199.9	200.1	-0.2	0.04
1254	228.0	226.3	1.7	2.89
1300	235.0	232.7	2.3	5.29
1577	285.0	271.2	13.8	190.44
1600	239.0	274.4	-35.4	1253.16
1750	293.0	295.2	-2.2	4.84
1800	285.0	302.1	-17.1	292.41
1870	365.0	311.8	53.2	2830.24
1935	295.0	320.8	-25.8	665.64
1948	290.0	322.6	-32.6	1062.76
2254	385.0	365.1	19.9	396.01
2600	505.0	413.1	91.9	8445.61
2800	425.0	440.9	-15.9	252.81
3000	415.0	468.6	-53.6	2872.96
			$\Sigma = 0$	$\Sigma = 18273.6$ = SSR

CHAPTER III

RESEARCH METHODOLOGY

This chapter presented processes for improving the manual counting process of P.Acne point using UV Fluorescence image by image processing. Research materials and tools such as MATLAB R2010a Program, IBM SPSS Statistics 20 Program, Adobe Photoshop CS5 Program, Microsoft Office, and Laptop were used. The important process is to compare manual process and automatic process. The details are as follows:

3.1 Research Methodology

Our research proposes method of automatically counting number of the P.Acne points using the UV Fluorescence and image processing. This method uses a process of image processing as follows. Cropping a UV image and selected a region of interest, then the cropped image (or the color image) is then used for a color processing to represent components of each image as three values including red, green, and blue color showing a value of global thresholding using Otsu's method. After that, find the optimal threshold (Automatic threshold) of selected layers of the color as shown in the histogram-threshold level. In addition, we have to make image adjustment by using Power-Law Transformation to determine the relative levels of gamma correction function in order to improve and adjust the P.Acne image and reduce noise within the images. Moreover, this process is related the optimal threshold for the purpose of analyzing and proving relevancy using regression equations. Next step is the image segmentation, by using the extended-maxima transform which allows binary image to be used for finding the difference between every pixel in a connection 8-ways and each pixel must be more than optimal threshold. This process sets to the H-maxima transform into a white color point called "object", but if it is less

than the level set to the H-maxima transform into a black color point called “background”. This helps to separate objects from the background automatically. Finally, counting the P.Acne point automatically by assigning number label and objects number, which help to specify points and calculate total points of all P.Acne of the image. It can be seen from figure.3.1 and Appendix B that the process could be described as follows.

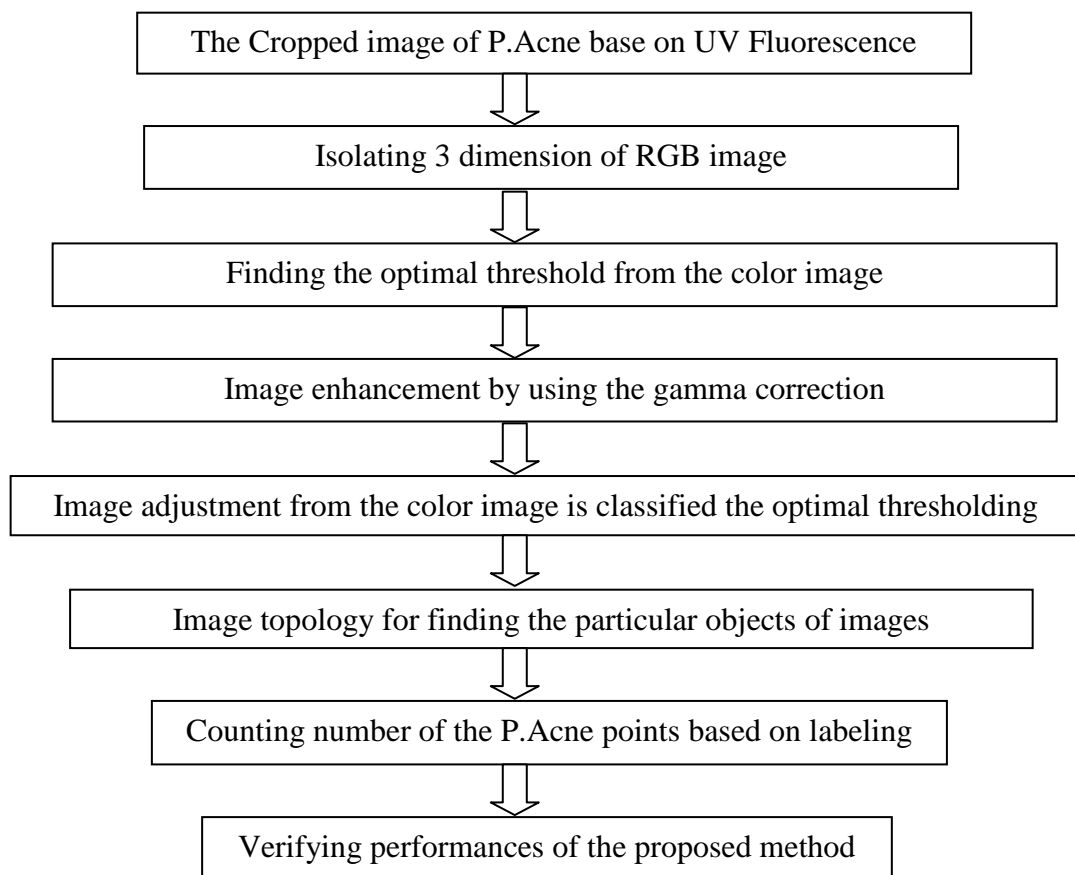


Figure 3.1 A proposed method of automatically counting number of the P.Acne Points using the UV Fluorescence and image processing

3.1.1 Color Image Processing

The color image requires three separate items of information for each pixel, a (true) color image of size $m \times n$ is represented in MATLAB by an array of size $m \times n \times 3$: a three dimensional array [17]. We can think of such an array as a single entity consisting of three separate matrices aligned vertically. Figure 3.2 shows a

diagram illustrating this idea. Suppose we read in an RGB image: We can isolate each color component by the colon operator:

$x(:, :, 1)$ The first, or red component

$x(:, :, 2)$ The second, or green component

$x(:, :, 3)$ The third, or blue component.

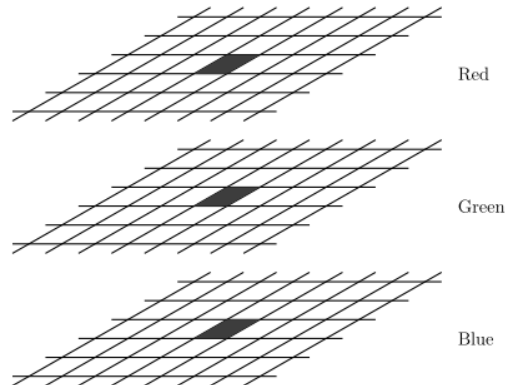


Figure 3.2 A three dimensional array for an RGB image

In our research the function below could be used in MATLAB to present the three dimensional as the command is presented in following:

```
I = imread('img0006-3.jpg'); %% input P.Acne image
figure, subplot(2,2,1), imshow(I), title('Original image') %Original
subplot(2,2,2), imshow(I(:, :, 1)), title('Red color') %R
subplot(2,2,3), imshow(I(:, :, 2)), title('Green color') %G
subplot(2,2,4), imshow(I(:, :, 3)), title('Blue color') %B
```

Also, it is separates the original color image of P.Acne in Figure 3.3 or it isolated each color component to three dimensional as shown in Figure 3.4.



Figure 3.3 An original color image of P.Acne

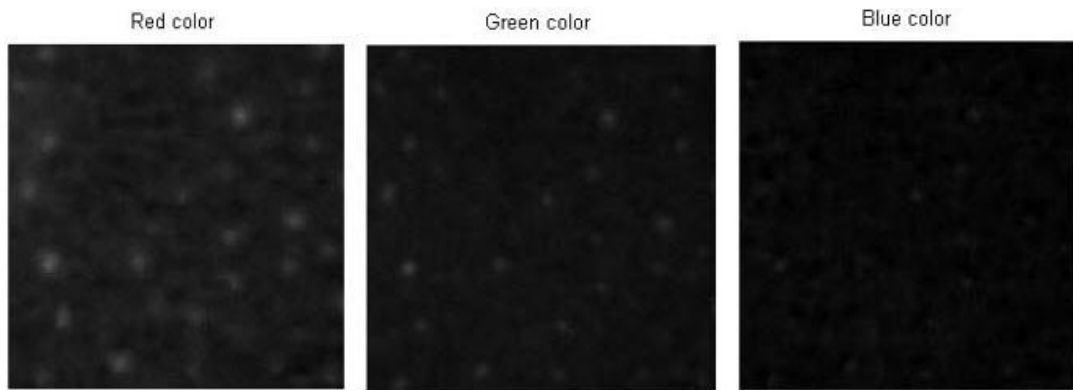


Figure 3.4 An RGB color image components of P.Acne

3.1.2 Global Thresholding

Reviewing previous process by classifying the objects in this research, threshold is divided 2 types such as Local thresholding and Global thresholding [18]. Function of thresholding is: $T = T[x, y, p(x, y), f(x, y)]$. In this research, most of global thresholding depends on $f(x, y)$, which uses only the gray level. Also, the selection threshold value of RGB image that referred to find the optimal threshold from the image is essential to running program by automatic thresholding that have two preferred methods such as Inter-means algorithm and Otsu's Method. Therefore, this research is used Otsu's Method because it has classified the information isolated of RGB image from three threshold values: Red, Green, and Blue Color. In the function of Otsu method in equations at (1) as follows:

$$\sigma^2(k) = P_0(m_0 - m)^2 + P_1(m_1 - m)^2 = P_0 P_1 (m_1 - m_0)^2 \quad (1)$$

Also, P_0 and P_1 is probability of data 2 groups $P_0 + P_1 = 1$, m_0 and m_1 is the mean value of each group, while m is the global mean value or $m = P_0 m_0 + P_1 m_1$.

In this technique, we used histogram to detect the P.Acne point and background of image. Then the program runs data to show threshold, each threshold isolated in RGB image and find the optimal threshold by Otsu's method in order to run command in MATLAB. The command is presented as follows:

```
I = imread('img0006-3.jpg'); %% input P.Acne image
th1= graythresh(I(:,:,1))
th2= graythresh(I(:,:,2))
th3= graythresh(I(:,:,3))
```

```

%%%Find max value of threshold From RGB Layer in image%%%
if(th1 > th2)&(th1 > th3)
    th_max = th1
    ia = I(:,:,1);
elseif (th2 > th1)&&(th2 > th3)
    th_max = th2
    ia = I(:,:,2);
elseif (th3 > th1)&&(th3 > th2)
    th_max = th3
    ia = I(:,:,3);
elseif (th1==th2)
    th_max = th1
    ia = I(:,:,1);
end

```

From this command, we described to find the optimal thresholding by automatic threshold and using 4 conditions as following;

- Red color threshold selected: $th1 > th2$ and $th1 > th3$
- Green color threshold selected: $th2 > th1$ and $th2 > th3$
- Blue color threshold selected: $th3 > th1$ and $th3 > th2$
- Red color threshold selected: $th1 = th2$

Because of the P.Acne point is reflex with UVF that appeared in the orange color light. The orange color light is close to two colors such as red and green color also, we are used conditions to run program by using these two colors. But if the green threshold equals to the red threshold, this program would be chosen the red color threshold because P.Acne points affects the UVF light and it is appears in the orange light which absorb light energy of the near ultraviolet (UV) and blue light energy [15]. Moreover, the blue color is blue light energy in the image that suitable for growing of P.Acne also, it is inessential for separating to select the P.Acne color point.

3.1.3 Image Enhancement

As previously stated the image enhancement is a process finding the power law response value called “Gamma correction” from an image and comparing with the threshold value, as stated in Appendix A. This relationship between input and output of gray level by Power-Law Transformation [24] is shown in function at (2) and graph in Figure 3.5.

$$s = cr^\gamma \quad (2)$$

$$s = cr^{1/3.0}$$

$$s = cr^{0.3}$$

S = output gray level

R = input gray level

C = the constant value of image (Almost, the value equals 1)

γ = Gamma correction (Normally, the gamma measurements is range from 1.0 to 3.0)

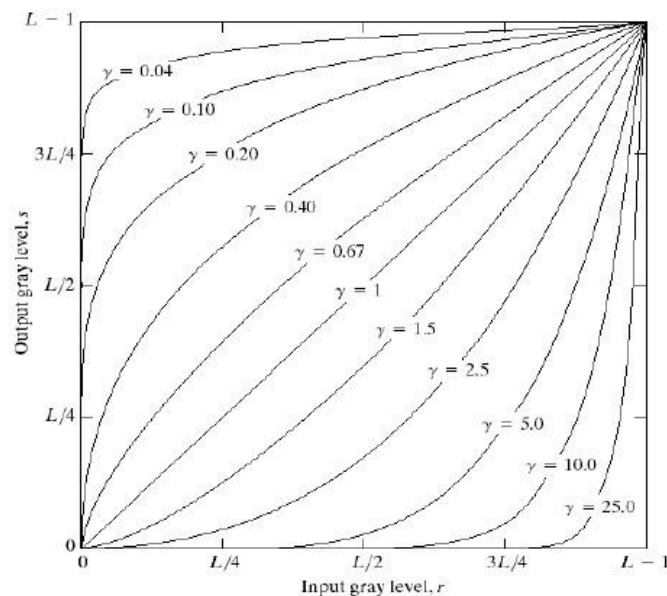


Figure 3.5 The gamma correction level by Power-Law Transformation

In this research, we are observed that if the optimal threshold that related with the gamma correction to input data for adjustment image is clearly. Also,

we can determine as same as stated in review papers [24] and show about the compared the gamma correction in 3 values from the P.Acne image such as 0.6, 0.4, and 0.3. Also, the best result is ranged approximately 0.3 is satisfy for improving contrast of the P.Acne image as follows Figure 3.6.

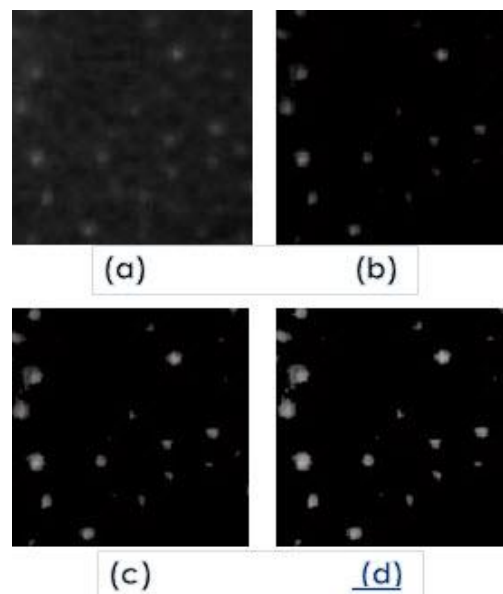


Figure 3.6 Improving contrast of the P.Acne image by gamma correction; (a) The original of P.Acne points image, (b) transformation with Gamma = 0.6, $c=1$, (c) transformation with Gamma = 0.4, $c=1$ (under acceptable level), (d) transformation with Gamma = 0.3, $c=1$ (best result)

In the observably, finding the gamma correction value from Power Law Transformation that is help to enhanced and adjusted the original image in image (A) more perfectly. However, we can distinguish the adjustment from image (Figure 3.6) and the value of threshold from histogram (Figure 3.7) as summaries of gamma correction in the best result of P.Acne image at 0.3. Nevertheless, the value of threshold comparing in the histogram of gamma correction such as 0.3, 0.4 and 0.6 has similarly the range of value in x-axis that is same trend in the histogram. Also, we are selected the value of gamma correction at 0.3, which this value would be used with imadjust function continuous.

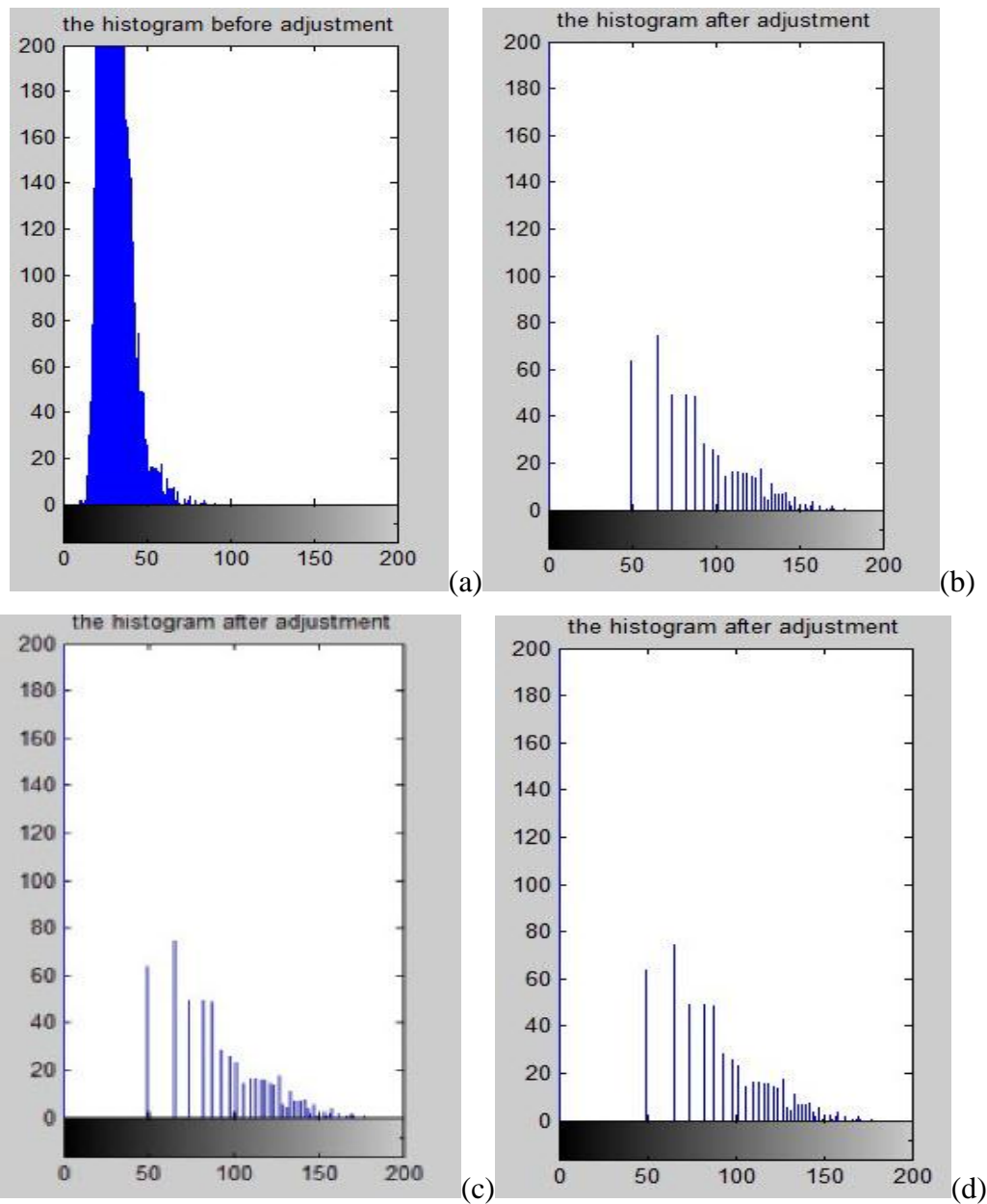


Figure 3.7 Histogram of the P.Acne image by gamma correction; (a) The original of P.Acne points image, (b) transformation with Gamma = 0.6, $c=1$, (c) transformation with Gamma = 0.4, $c=1$ (under acceptable level), (d) transformation with Gamma = 0.3, $c=1$ (best result)

Therefore, we used the sample regression analysis model called “Linear equation” to prove this relationship. From our experiment information, we used scatter plot from IBM SPSS Statistic20 to run 50 samples from using correlations value of the

value of threshold between the optimal threshold of color image and the low-input value of imadjust function in Figure 3.8. From descriptive statistic in Table 3.1, our research shows the value of mean and standard deviation of the optimal threshold and the low-input value of imadjust function.

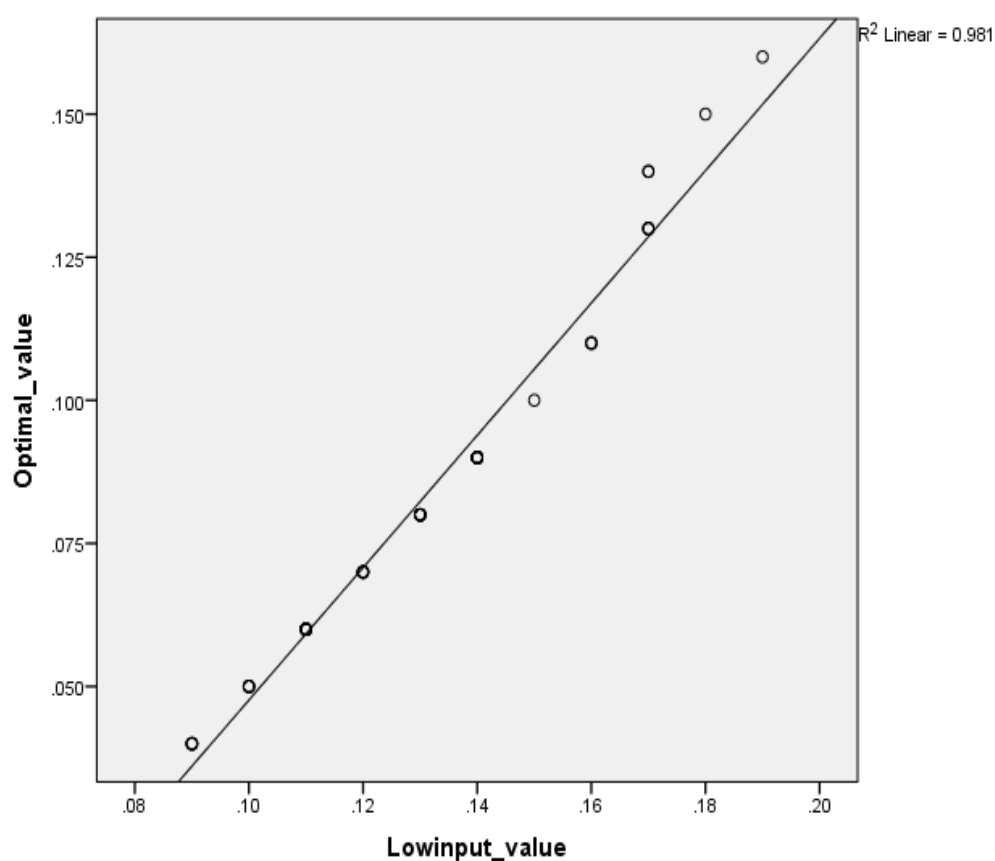


Figure 3.8 The linear regression between the optimal threshold and the Low input value of imadjust function of P.Acne points

Table 3.1 The descriptive statistics

Descriptive Statistics			
	Mean	Std. Deviation	N
Optimal value	.0814	.03010	50
Low-input value	.1292	.02578	50

Table 3.2 The regression model summary**Model Summary**

Model	R	R Square	Adjusted R Square	Std. Error of the Estimate	Durbin-Watson
1	.990 ^a	.981	.980	.00424	1.874

a. Predictors: (Constant), Low-input value

b. Dependent Variable: Optimal value

Table 3.3 The Coefficients Model**Coefficients^a**

Model	Unstandardized Coefficients		Standardized Coefficients	t	Sig.	95.0% Confidence Interval for B	
	B	Std. Error	Beta			Lower Bound	Upper Bound
(Constant)	-.068	.003		-21.969	.000	-.074	-.062
Low-input value	1.156	.023	.990	49.207	.000	1.109	1.203

a. Dependent Variable: the optimal value

Then, our research proved this relationship by regression equation or Linear equation, where we calculated coefficients model as shown in Table 3.3. The following function was used as our linear equation at (3).

$$Y = a + bX \quad (3)$$

$$Y = -0.68 + 0.981(1.156)$$

$$Y = 0.454$$

a=constant is intercept of regression

b=slope/Coefficient of Regression (R²)

X=Predictor (Constant)

Therefore, the result of regression equation is 0.454, R Square is 0.981 or 98.1 %, follows the model summary in Tables 3.2 showing the bound of $0 \leq R^2 \leq 1$. This is for the purpose of having the coefficient of correlation value close to 1. Moreover, it has a positive relationship, which specify the goodness of fit as per the review paper [25] and can support the following hypothesis:

$$H_0 : \beta_1 = \beta_{1,0} = 0 \quad (4)$$

$$H_1 : \beta_1 \neq \beta_{1,0} \neq 0 \quad (5)$$

Also, this research would reject the hypothesis 0 in equations at (4), but accepts hypothesis 1 in equations at (5). This indicates that there is a relationship between the optimal threshold of color image and the Low input value of imadjust function. This is due to the fact that we analyze the two relationships by bivariate correlation as shown in Table 3.4. Afterwards, we analyze the two relationship variables: The Pearson Correlation of max value, such as max value and max value that equals 1 because it has related with itself and max value and gamma value that equals 0.990. Also, the value is close to 1 which shows the strongest relationship in same direction, so that the interval of this value is between zero to one which is a positive value. As seen in table 3.4, the Pearson correlation of Low-input value of imadjust function shows the strongest relationship, as it is the same as the value of the optimal threshold of Pearson correlation.

Table 3.4 The bivariate correlations table**Correlations**

		Optimal value	Low_input value
<u>Optimal value</u>	<u>Pearson Correlation</u>	<u>1</u>	<u>.990^{**}</u>
	Sig. (2-tailed)		.000
	Sum of Squares and Cross-products	.044	.038
	Covariance	.001	.001
	N	50	50
<u>Low_input value</u>	<u>Pearson Correlation</u>	<u>.990^{**}</u>	<u>1</u>
	Sig. (2-tailed)	.000	
	Sum of Squares and Cross-products	.038	.033
	Covariance	.001	.001
	N	50	50

^{**}. Correlation is significant at the 0.01 level (2-tailed).

3.1.4 Histograms

This research used histogram to compare the threshold value for improving the image. The histogram consists of the gray levels and an indication of number of times each gray level occurs the image [17]. We can deduce that the appearance of an image from the histogram, as per following example, indicates: In a dark image; the gray levels would be clustered at the lower end. In a uniformly bright image; the gray levels would be clustered at the upper end. In a well-contrasted image; the gray levels would be well spread out over much of the range [Book]. Also, we can view the histogram before and after adjustment of the P.Acne image by using the following imhist function and this command is presented,

```
I = imread('img0006-3.jpg');
imshow(I,title('Histogram of P.Acne Image'))
```

The result is shown in Figure 3.9. From the observed histogram; the gray values are all clustered together in the center of the histogram, also the image is poorly contrasted. Then we enhanced this contrast by spreading out its histogram by using histogram stretching (contrast stretching) because this method is suitable for the P.Acne image.

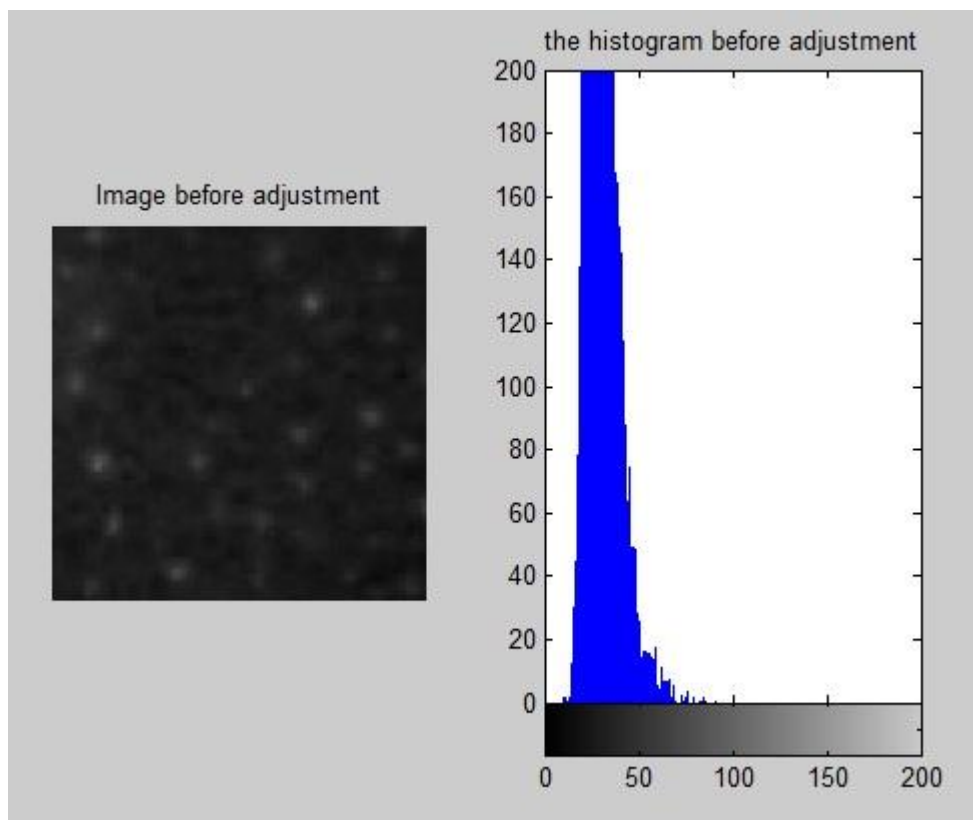


Figure 3.9 Histogram of the original of P.Acne image

3.1.4.1 Histogram Stretching (Contrast Stretching)

This Research can stretch out the gray levels in the object range by applying the `imadjust` function below:

`Imadjust (im, [a, b], [c,d])`

Using this command would stretch the image according to the function shown in Figure 3.10. Because `imadjust` is designed to work equally well on images of type `double`, `uint8`, or `uint16`. The values of a , b , c , and d must be between 0 and 1; the

function automatically converts the image (if needed) to be of type double [17]. In addition, the `imadjust` does not work quite in the same way as shown in Figure 3.8, if pixel values are less than all would be converted to c , and if pixel values are greater than b all would be converted to d .

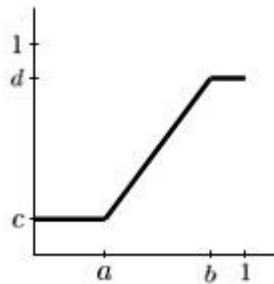


Figure 3.10 The stretching function given by `imadjust`

The `imadjust` function has one other optional parameter: the gamma value, which describes the shape of the function between the coordinates (a, c) and (b, d) . If gamma is equal to 1, which is default, then a linear mapping is used, as shown in Figure 3.8. However, values less than 1 produce a function that is concave downward, as shown on the left in Figure 3.11, and value greater than 1 produce a figure that is concave upward, as shown on the right in Figure 3.11.

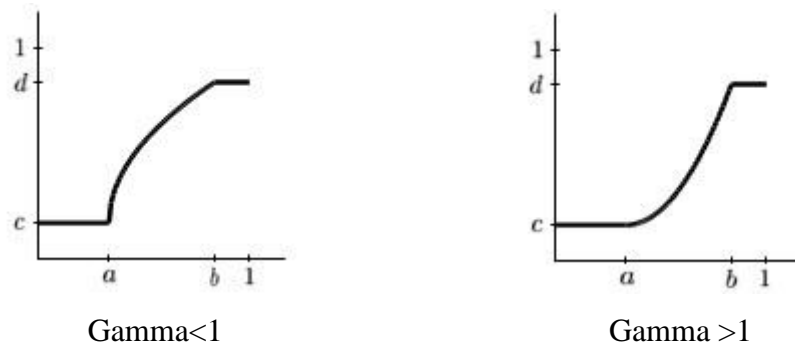


Figure 3.11 The `imadjust` function with gamma not equal to 1

This research used the gamma value equals 0.3 which is values less 1 produce a function that is concave downward and enough to improve the appearance of the P.Acne and then show comparison between before adjustment and after adjustment of the P.Acne image (Figure 3.12). This command is presented as follows,

```
I = imread('img0006-3.jpg');
ia = I(:,:,1);
```

```

%% find value from the optimal threshold of image
lowinput = low_in;
%%find value from relationship of the gamma correction
ia2= imadjust(ia,[low_input 0.8],[0 1],0.3)
subplot(2,2,1), imshow(ia),title('Image before adjustment')
subplot(2,2,2), imhist(ia),title('the histogram before adjustment')
subplot(2,2,3), imshow(ia2),title('Image after adjustment add gamma')
subplot(2,2,4), imhist(ia2),title('the histogram after adjustment')

```

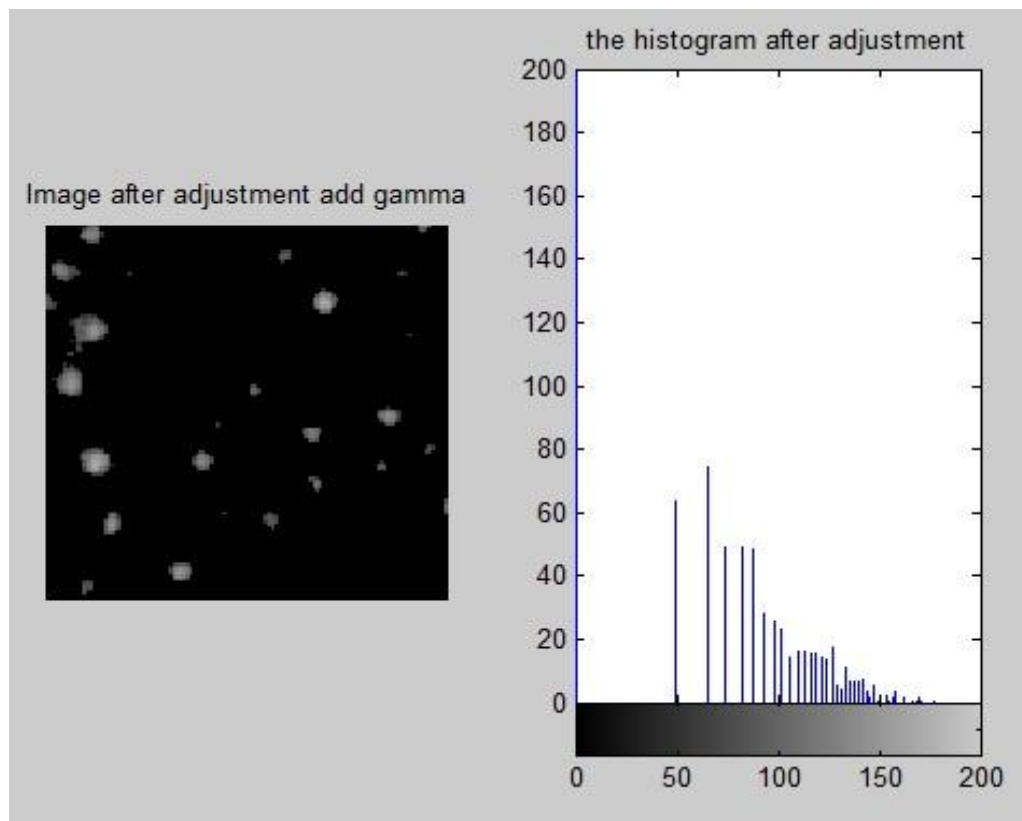


Figure 3.12 The P.Acne image before and after adjustment by imadjust function

From figure 3.12, the histogram of P.Acne image has the threshold value close to 200 or it has expanding to the right side of x-axis in nearly the white color. Also, the imadjust function is decreased noise from the original image by contrasting the optimal threshold of image. Moreover, this process can applied for improving the P.Acne image is more clearly.

3.1.5 Image Topology

This research would focus on the number of occurrences of a particular object, P.Acne points. The investigation of these fundamental properties of an image is called digital topology or image topology [17]. Also, the counting number of P.Acne Point used the function of Extended H-maxima Transform and function labeling because of P.Acne points is very small point, with different sizes, unclear points, and dark background. Therefore, this function solved problem regarding difficulty in counting and making the labels in each P.Acne point. This has increased efficiency and saves time in counting and analyzing.

3.1.5.1 Extended Maxima transform

The extended-maxima transform is the regional maxima of the H-maxima transform. H is nonnegative scalar [17]. Regional maxima are connected components of pixels with a constant intensity value, and whose external boundary pixels all have a lower value. By default, `imextendedmax` uses 8-connected neighborhoods for 2-D images and 26-connected neighborhoods for 3-D images, with the function as follows.

BW = imextendedmax(I,H)

This function helps to separate the objects and other objects when they are close to one another. Algorithm of the regional maxima is a method for connecting components of pixels with a constant intensity value, and whose external boundary pixels have lower values [16]. Maxima means object which is white in color. Background is black in color. In this research, we applied the pre-adjusted P.Acne image and the optimal threshold value with the as follows above function and this command is presented;

```
th_check= roundn(th_max, -2);
ia2 = imadjust(ia,[low_input 0.8],[0 1],0.3);
bw = imextendedmax(ia2, th_check);
```

As a result from the process of extended maxima transform, the output result and the histogram from Figure 3.13 will then be used for labeling method, marking number of the P.Acne points.

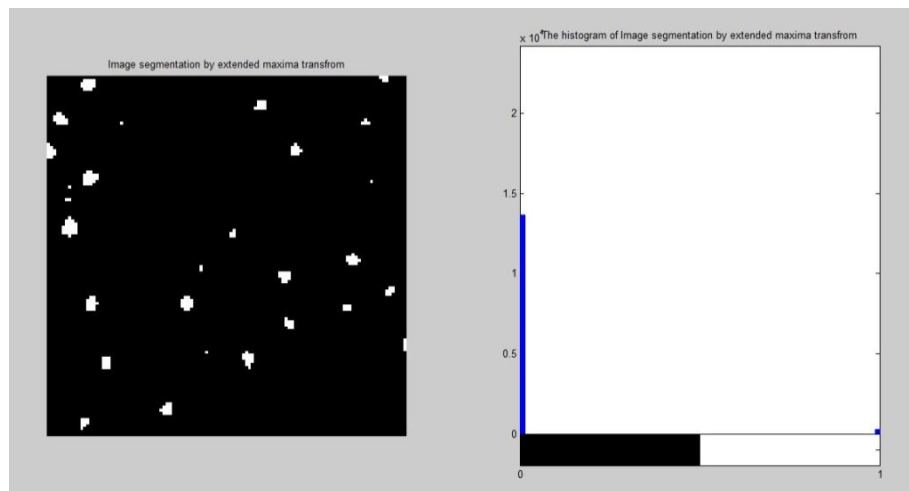


Figure 3.13 The image and histogram resulted from Extended H-Maxima Transform

This method considers the importance “middle ground” between individual foreground pixels and the set of all foreground pixels [16]. The connection of each component is defined in terms of a path and the definition of the path, depending on the adjacency. This method chooses an 8-adjacency for a mask of image [16].

3.1.5.2 Labeling

In labeling, the label connected components in 2-D binary image uses the function as follows:

$$[L, \text{num}] = \text{bwlabel}(BW, n)$$

The variable of this function such as BW is a variable n, which could have a value of either 4 or 8, where 4 specifies 4-connected objects and 8 specifies 8-connected objects [17]. If the argument is omitted, it would be at default value of 8. The elements of L are integer values greater than or equal to 0. The pixels labeled 0 are the background. The pixels labeled 1 make up one object. The pixels labeled 2 make up a second object, and so on. In addition, the variable num is the number of connected objects found in BW. Also, we applied the following function in our research and this command is presented;

```

%%% Counting Number %%%
[L2,n] = bwlabel(bw);
figure,subplot(1,3,1),imshow(O),title('Show image by manual process')
subplot(1,3,2),imshow(I),title('Show Original image')
subplot(1,3,3),imshow(bw),title('Show image by Image processing');
hold on
for i=1:n
    [r,c]=find(L2==i);
    text(mean(c),mean(r),num2str(i),'color','red');
end
countacne = n
%%% Show the total of number P.Acne point of automatic counting %%%

```

By using the labeling function, it is easier to count the number of P.Acne point and save more time as marking the number of point is fast. As shown in Figure 3.12 the counting on the left, this image is an example of the result for manually counting of number of the P.Acne points. While on the right in Figure 3.12 shows an example of the result of automatic counting of the P.Acne points using image processing and the labeling method. Also, this is a clear comparison of the process of counting number of P.Acne points between manual process and auto process of an images of P.Acne images in show in Appendix B.

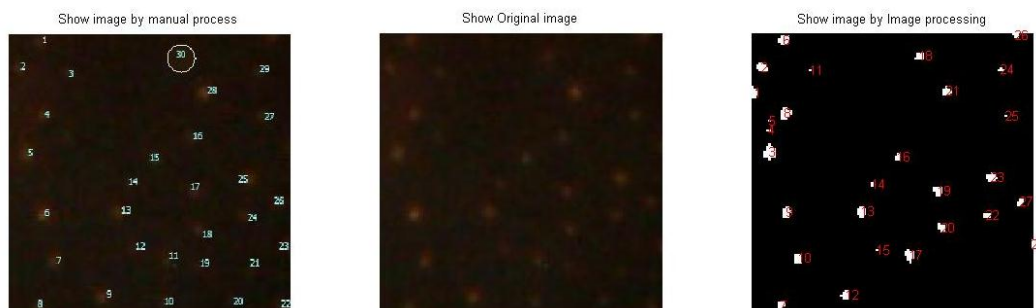


Figure 13.14 Results comparing between the manual and the automatic counting number of P.Acne points using labeling method.

3.2 Verification of performances

In Table 3.5, the verification of the P.Acne points for the proposed method is shown. This measured in terms of four values (1) The true positive (TP) rate (number of the P.Acne Points correctly detected). (2) The false positive (FP) rate (number of non-P.Acne points wrongly detected as the P.Acne points). (3) The false negative (FN) rate (number of the P.Acne points not detected). (4) The true negative (TN) rate (number of non- P.Acne points correctly identified as non- P.Acne points). This research used three indicators to verify the performances in the proposed method as follows: Firstly, accuracy; the overall successful rate of counting number of the P.Acne points. Secondly, sensitivity; the percentage of the actual P.Acne points that are detected. Thirdly, precision; the accurate percentage of the actual P.Acne points that are detected. From these quantities, accuracy, sensitivity and precision are defined as equations (6), (7) and (8), respectively.

Table 3.5 The Verification of the P.Acne

	The Proposed Method	
	Present	Absent
Positive	True Positive (TP)	False Positive (FP)
Negative	False Negative (FN)	True Negative (TN)

$$\text{Accuracy} = (TP+TN)/(TP+TN+FP+FN) \quad (6)$$

$$\text{Sensitivity} = TP/(TP+FN) \quad (7)$$

$$\text{Precision} = TP/(TP+FP) \quad (8)$$

This chapter presented the methodology of image processing from first step until final step, which composed of Isolate 3 dimensions of RGB image, finding the optimal threshold and classifying by Otsu's method, image enhancement by

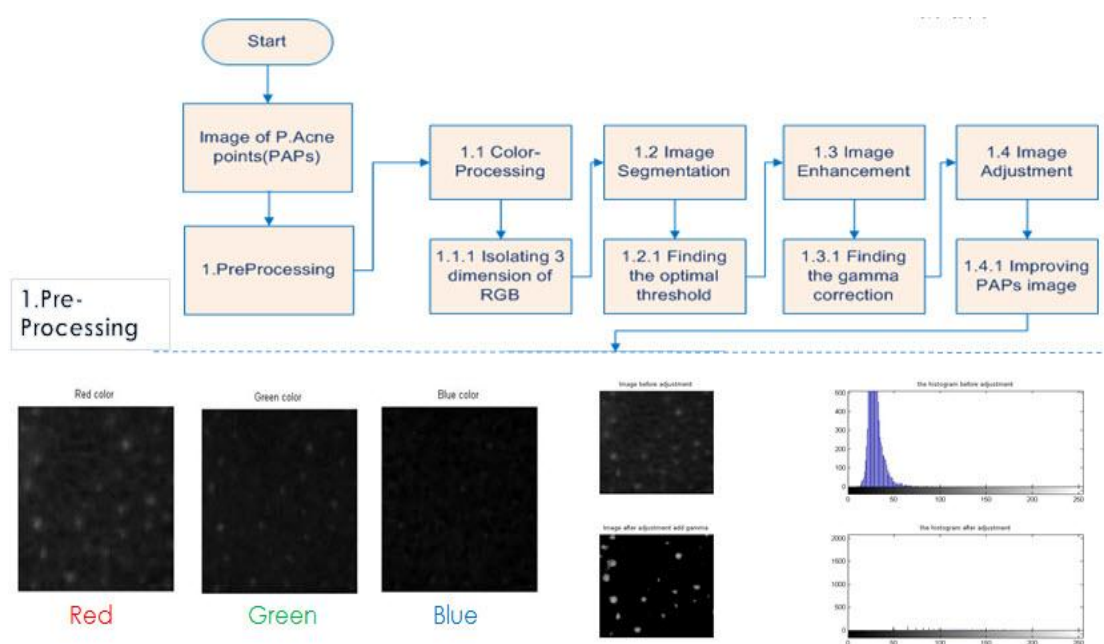
gamma correction using Power-Law Transformation, image adjustment, and image topology for finding, counting number of the objects and verification of performances.

In the paper review, almost of counting methods are used the matrix confusion for applied the verify data because it is help to find the accuracy for detection the truth objects and assess the quality of the proposed method as follows; counting method in fluorescence microscopy image [23]: they are used the measures of precision(P), recall(R) and F-measure(F) as defined that $P = tp / (tp + fp)$, $R = tp / (tp + fn)$, and $F = (2.P.R) / (P + R)$, where tp(true positive) is the number of items labeled correctly as cell, fp(false positives) is the number of items classified incorrectly by the method as cell, and fn(false negatives) is the number of items that were not classified as cell but should have been. They evaluated each image counted using the proposed method by point out the cells that were not counted (false negatives) and artifacts that were incorrectly classified as cells (false positive). Also, we are applied this verification of evaluate method for measurement of performance between manual processing and image processing we are described this process in next chapter. The next chapter presents the average of performance values and comparing the results of this research, using method stated above to improve and analyze 50 patients by using the P.Acne image from Institute of Dermatology.

CHAPTER IV

RESULTS AND DISCUSSION

This research gathered the Acne patient of 50 persons from Bio Engineering Laboratory unit of Dermatology. In Preprocessing, the medical specialist of Dermatology operates the research and cooperates with the medical technician of the bioengineering unit of Dermatology that plans and tests the growing rate of the P.Acne. In the experiment, the number of the acne points is counted by human eye from images based on the VISIA camera i.e. a photo of UV Fluorescence that helps to see the image more clearly and to count them. However, there are many problems in counting high number of them due to possible inaccuracy as the acne image is difficult to analyze and distinguish the acne points. Also, the human eye cannot see the acne image clearly in some surface, as a result; they may make a mistake in analyzing and consume approximately 5 minutes per image. This research presents counting number of points of acne vagaries using UV Fluorescence and image processing. We have to introduce a major process of image processing are three steps in figure 4.1.



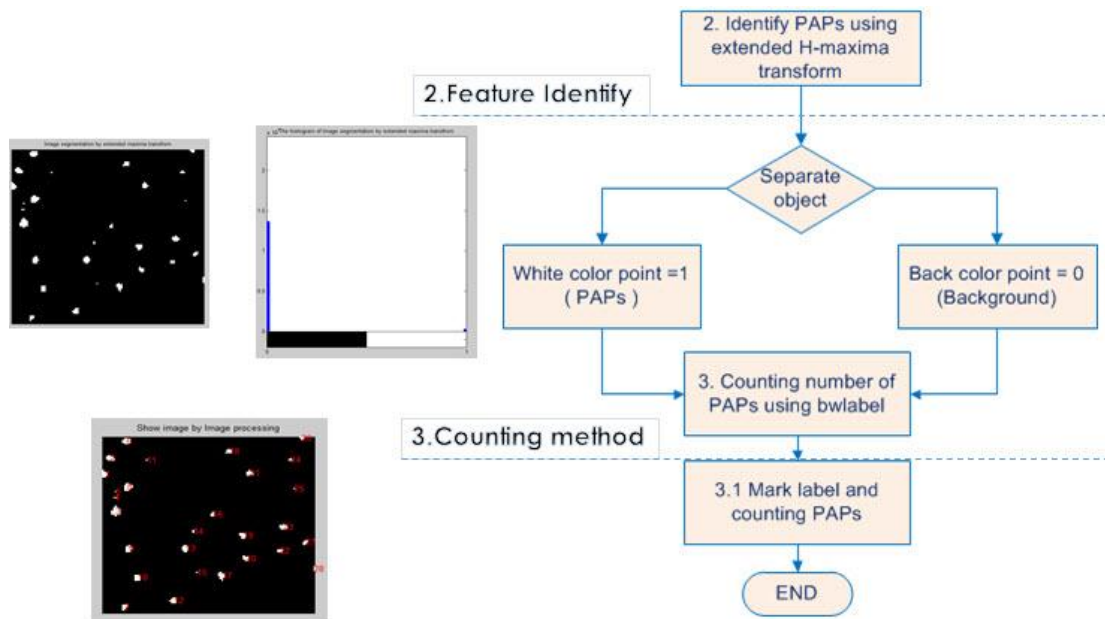


Figure 4.1 The chart diagram of three major methods of P.Acne counting by using image processing

From figure 4.1, we are described above processes as follows: First, pre-processing step such as color processing to represent components of each image into three values including RGB color indicated a value of global threshold by Otsu's method, finding the optimal threshold (Automatic threshold) of selected layers of color image as shown in the histogram-threshold level, enhancing image by Power-Law Transformation to determine the relative levels of gamma correction function for improving and adjusting the P.Acne image and reduce the noise within the images that corresponds to the optimal of threshold for the purpose of analyzing and proving relevancy using regression equations. Second, feature identification step is segmented of image by using the extended H-maxima transform which allows binary image to be used for finding the difference between every pixel in a connection 8-ways as each pixel must be more than optimal threshold. This would help automatically separating objects from the background. Third, counting method is automatic counting by assigning number label and object number, which help to specify points and calculate total points of P.Acne image. This chapter presents the process of verification of performances on counting the P.Acne point by using image processing.

4.1 Verification of performances by image processing

From the experimental results, fifty images of the P.Acne points were used for testing on the proposed method based on the MATLAB program. Table 4.1 shows the results of counting number of PAPs comparing between human eye and image processing. Table 4.2 shows the overall results of performances in terms of three indicators i.e. accuracy, sensitivity and precision, respectively.

Table 4.1 The results of counting number of the P.Acne points, comparing between methods of human eye and image processing.

The results of counting number of The P.Acne Points						
P.Acne Image	Real (Human)	Output (Computer)	True Positive	False Positive	True Negative	False Negative
DATA1	47	49	47	2	-	0
DATA2	36	38	36	2	-	0
DATA3	25	28	25	3	-	0
DATA4	35	33	33	0	-	2
DATA5	30	28	28	0	-	2
DATA6	40	38	38	0	-	2
DATA7	22	20	20	0	-	2
DATA8	24	19	19	0	-	5
DATA9	27	26	26	0	-	1
DATA10	77	80	77	3	-	0
DATA11	20	15	15	0	-	5
DATA12	13	12	12	0	-	1
DATA13	49	51	43	2	-	0
DATA14	52	57	52	5	-	0
DATA15	18	12	12	0	-	6
DATA16	63	63	63	0	-	0
DATA17	52	56	52	4	-	0
DATA18	40	40	40	0	-	0
DATA19	45	49	45	4	-	0
DATA20	52	49	49	0	-	3
DATA21	20	16	16	0	-	4
DATA22	15	11	11	0	-	4
DATA23	36	37	36	1	-	0
DATA24	25	20	20	0	-	5
DATA25	35	31	31	0	-	4
DATA26	35	32	32	0	-	3
DATA27	69	67	67	0	-	2
DATA28	24	20	20	0	-	4

P.Acne Image	Real (Human)	Output (Computer)	True Positive	False Positive	True Negative	False Negative
DATA29	45	44	44	0	-	1
DATA30	15	15	15	0	-	0
DATA31	11	16	11	5	-	0
DATA32	12	17	12	5	-	0
DATA33	41	41	41	0	-	0
DATA34	11	13	11	2	-	0
DATA35	39	35	35	0	-	4
DATA36	11	13	11	2	-	0
DATA37	60	62	60	2	-	0
DATA38	119	123	119	4	-	0
DATA39	8	10	8	2	-	0
DATA40	63	62	62	0	-	1
DATA41	48	48	48	0	-	0
DATA42	33	28	28	0	-	5
DATA43	85	84	84	0	-	1
DATA44	22	26	22	4	-	0
DATA45	25	21	21	0	-	4
DATA46	11	9	9	0	-	2
DATA47	37	36	36	0	-	1
DATA48	21	18	18	0	-	3
DATA49	22	24	22	2	-	0
DATA50	56	61	56	5	-	0
TOTAL	1821	1803	1738	59	-	77

Therefore, in table 4.1 shows the result of the P.Acne points for the proposed method which is measured in terms of four values as (1) the true positive (TP) rate (number of the P.Acne Points correctly detected), (2) the false positive (FP) rate (number of non-P.Acne points wrongly detected as the P.Acne points), (3) the false negative (FN) rate (number of the P.Acne points not detected) and (4) the true negative (TN) rate (number of non- P.Acne points correctly identified as non- P.Acne points). This research is used three indicators to verify the performances in this proposed method as follows. Firstly, accuracy is the overall successful rate of counting number of the P.Acne points. Secondly, sensitivity is the percentage of the actual P.Acne points that are detected. Thirdly, precision is the accurate percentage of the actual P.Acne points that are detected. Also, the experiment on 50 samples of P.Acne images results are shown in table 4.2. This show the accuracy, sensitivity, and precision of approximately at 92.45%, 95.76% and 96.39%, respectively.

Table 4.2 The overall results of performances in terms of three indicators i.e. accuracy, sensitivity and precision.

Indicators type	Formula of matrix fusion	Total Average
ACCURACY	$(TP+TN)/(TP+TN+FP+FN)$	92.74%
RECALL	$TP/(TP+FN)$	95.76%
PRECISION	$TP/(TP+FP)$	96.72%

Furthermore, counting number of P.Acne point by using image processing method can save time to analyze of the P.Acne image more effectively. Shown in table 4.3 is the comparisons of methods between manual processing and image processing. Appendix B contains 50 pictures of the P.Acne image samples comparing between manual processing and image processing to achieve a better understanding of the operational characteristics of P.Acne points including the possibility of finding the position of the P.Acne points by image processing.

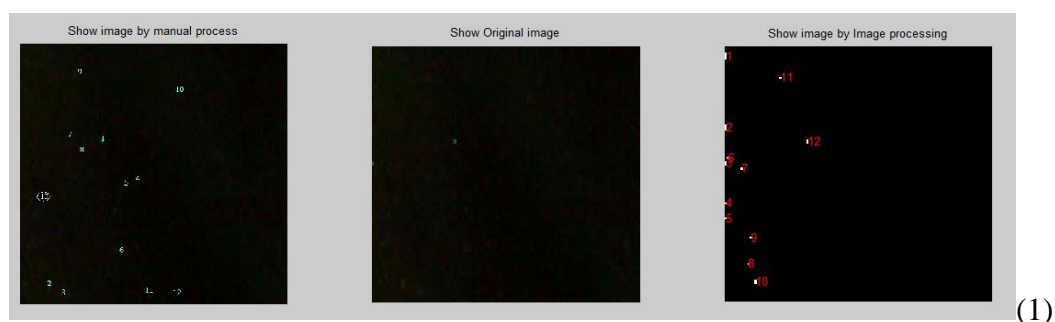
Table 4.3 The comparing counting method between manual processing and image processing

Details	Manual Processing	Image Processing
Time duration	≥ 5 minutes/image	5 seconds/image
Count Tool	Mark Label from Photoshop Program	Automatic Label from MATLAB Program
Detection P.Acne Points	Human Eye (Vision)	Image processing(Automatic) such as Color processing, Image Enhancement, Image Adjustment, and Image Topology
Counting recheck	Medical Technician	Automatic comparing the PAPs image
Theory support	Expert Skill	Otsu's method Power –Law transformation Sample Regression Analysis
Analysis Level	Difficult	Easy
Task	More labor	A labor to control program
Image	Not clear, Burr	Clear and not burr

This chapter presents the result of image processing of P.Acne image for counting P.Acne points with the methodology state in chapter three, the final result of this chapter is the verification of performances of the P.Acne point counting by using image processing, which can help to analyze the P.Acne point and reduce time in counting. The next chapter presents the discussion of this research's finding and methodology used.

4.2 Discussion of counting P.Acne points by image processing

From the international conference, we are developed from gray image to color image by image processing to distinguish P.Acne point. Also, the result of accuracy is more than 90 %. Although, the result of this analysis is with higher accuracy, but error appears in some images due to the fact that Acne patient images were taken from the LAB which has changing environment. The difference in the patient's skin conditions may have caused errors as well. This result in the P.Acne points in UVF image affects the color and it is not uniform so it is difficult to diagnose. While we observed, the experimental pictures with more points is burred, and mixed substance in the seven images such as Data 12, 13, 18, 19, 25, 34 and 43 (Figure 4.1). All of the threshold values from 50 samples of P.Acne image is shown in Table 4.4, respectively.





(2)



(3)



(4)



(5)



(6)



Figure 4.2 Seven samples image: 12(1), 13(2), 18(3), 19(4), 25(5), 34(6) and 43(7)
show missing the P.Acne points

Table 4.4 The value threshold of P.Acne image of 50 samples

Sample image	Red color threshold	Green color threshold	Blue color threshold	Optimal threshold	Low-input threshold
Data1	0.1412	0.0902	0.0431	0.14	0.17
Data2	0.1020	0.1294	0.0627	0.13	0.17
Data3	0.0941	0.0706	0.0314	0.09	0.14
Data4	0.1490	0.0824	0.0431	0.15	0.18
Data5	0.1333	0.0745	0.0353	0.13	0.17
Data6	0.1373	0.1373	0.0588	0.14	0.17
Data7	0.0824	0.0745	0.0275	0.08	0.13
Data8	0.0980	0.1333	0.0471	0.13	0.17
Data9	0.1020	0.1137	0.0667	0.11	0.16
Data10	0.1647	0.1490	0.1098	0.16	0.19
Data11	0.0627	0.0627	0.0196	0.06	0.11
Data12	0.0392	0.0353	0.0078	0.04	0.09
Data13	0.0863	0.0824	0.0275	0.09	0.14
Data14	0.0863	0.0667	0.0314	0.09	0.14
Data15	0.0706	0.0902	0.0471	0.09	0.14
Data16	0.0667	0.0902	0.0471	0.09	0.14
Data17	0.0706	0.0941	0.0510	0.09	0.14
Data18	0.0510	0.0549	0.0314	0.05	0.10
Data19	0.0706	0.0745	0.0275	0.07	0.12
Data20	0.0824	0.0745	0.0275	0.08	0.13
Data21	0.0392	0.0431	0.0157	0.04	0.09
Data22	0.0549	0.0549	0.0196	0.05	0.10
Data23	0.0588	0.0627	0.0275	0.06	0.11
Data24	0.0549	0.0549	0.0196	0.05	0.10
Data25	0.0627	0.0667	0.0275	0.07	0.12
Data26	0.0392	0.0431	0.0157	0.04	0.09
Data27	0.0824	0.0549	0.0235	0.08	0.13

Sample image	Red color threshold	Green color threshold	Blue color threshold	Optimal threshold	Low-input threshold
Data28	0.0784	0.0471	0.0196	0.08	0.13
Data29	0.0902	0.0549	0.0235	0.09	0.14
Data30	0.0588	0.1059	0.0706	0.11	0.16
Data31	0.0431	0.0431	0.0157	0.04	0.09
Data32	0.0627	0.0588	0.0196	0.06	0.11
Data33	0.0784	0.0627	0.0235	0.08	0.13
Data34	0.0784	0.0745	0.0275	0.08	0.13
Data35	0.0980	0.0824	0.0275	0.10	0.15
Data36	0.0588	0.0471	0.0157	0.06	0.11
Data37	0.0706	0.0627	0.0235	0.07	0.12
Data38	0.1137	0.0784	0.0353	0.11	0.16
Data39	0.0667	0.0510	0.0196	0.07	0.12
Data40	0.0706	0.0941	0.0431	0.09	0.14
Data41	0.0667	0.0706	0.0275	0.07	0.12
Data42	0.0824	0.0824	0.0392	0.08	0.13
Data43	0.0510	0.0588	0.0275	0.06	0.11
Data44	0.0627	0.0431	0.0157	0.06	0.11
Data45	0.0627	0.0471	0.0157	0.06	0.11
Data46	0.0588	0.0392	0.0118	0.06	0.11
Data47	0.0627	0.0471	0.0157	0.06	0.11
Data48	0.0627	0.0431	0.0196	0.06	0.11
Data49	0.0549	0.0392	0.0157	0.05	0.10
Data50	0.0745	0.0471	0.0196	0.07	0.12

The results of seven images from this table were observed the thresholds of the images are similar, for example; the Red and Green dimensions. Also, the threshold values are related with findings of the P.Acne points from the image. However, we might be able to find more methods from the image processing to apply with the classification of this group for improving image and detect point with higher precision and efficiency in the future work. This chapter discussed the research topics with other researches in many subjects such as the opinion bias of the oral presentation, and testing more samples of the experiment. Next chapter concludes the research and recommends for future study.

CHAPTER V

CONCLUSION AND RECOMMENDATION

5.1 Conclusion

The proposed method can count the number of the PAPs using the UVF and image processing. The result shows that the accuracy, sensitivity and precision are approximately at 92.45%, 95.76% and 96.39%, respectively. The image processing can clearly help to improve the acne image for suitable analysis method and count the total number of acne vulgaris points. It also saves the time in counting, recording and sending the data for the doctor analysis. In this research, the image processing is modified the manual counting method of P.Acne point, which is suitable for specifying the P.Acne point quickly and efficiently. In summary, the advantage of this research finding is that it decreases the mistakes of manual counting by using the Acne patient's image with UV Fluorescent light. This improved the manual counting method to become easier, comfortable, and specification of interested object is more clearly. Also, it can help as this process saves time in counting P.Acne point and reduce the counting task of medical technician, so it reduces the waiting time of the result in the Bioengineering Laboratory. Therefore, the result of counting number of P.Acne points helps increase in efficiency analyzing and diagnosing process of the Acne patient because the medical doctor can analyze the growing rate whether increased it or decreased within the duration, a comparison before and after the acne treatment from having future acne vulgaris. The treatment will help to prevent the acne patients.

5.2 Recommendation

5.2.1 Image processing technique improvement

This research describes the image processing, which focuses on detecting the P.Acne points. The result depends on the feature and the color of P.Acne image. The limitation of this research is the quality of image and environment while the photo was taken in the Laboratory. Further study should include developing image processing and gathering method such as; enhancing the quality of image, finding the missing errors, classify the point more accurately, and testing more samples to develop the program in the future work.

REFERENCES

- 1 Institute of Dermatology, <http://www.inderm.go.th>.
- 2 K. Preeya, and P. Prawit, Acne disease magazine, 2010.
- 4 T. Wirat, Doctor magazine, 2005.
- 5 H. Mohammad, “Automatic Counting of Leukocytes in Giemsa-Stained Images of Peripheral Blood Smear,” Iran, 2009.
- 6 Clayton M. Costa, “Counting pollen grains using readily available, free image processing and analysis software,” USA , 2009.
- 7 Z. Ping, “Grain Counting Method Based On Image Processing,” China, 2009.
- 8 P. Wijethunga, “Digital Image Analysis Based Automated Kiwifruit Counting Technique,” New Zealand, 2008.
- 9 Y. H. Toh, “Automated fish counting using image processing,” Singapore.
- 10 F. Andrés, “Peruvian Scallop Larvae counting system using image processing techniques,” Peru, 2008.
- 11 M. Hong, “Counting Method of Heterotrophic Bacteria Based on Image Processing,” China, 2008.
- 12 S. Wei-zheng, “Experimental Study for Automatic Colony counting System Based on Image Processing,” China, 2010.
- 13 X. Pengyun, “Computer assistance image processing spores counting,” China, 2009.
- 14 H. Fujii, “Extraction of acne lesion in acne patients from multispectral images,” Japan, 2008.
- 15 Bluhm, and Hollman, “Acne and rosacea book 2 nd, completely revised and enlarged editin with a contribution,” 1975, pp. 70-74.
- 16 Sec I, Fluorecence spectroscopy for endogenous porphyrins in human facial skin: SPIE, 2009.
- 17 Alasdair McAndrew, “Digital Image Processing with MATLAB”; 2004.18 BS 7799 Becomes ISO 27001. BH Consulting. 2005

- 18 Yuttapong Rangsanteri, Pornphan Dulyakarn, Image Segmentation Using Multithresholding of Second-Order Gray-Level Statistics, Department of Telecommunications Engineering, Faculty of Engineering , King Mongkut's Institute of Technology Ladkrabang.
- 19 J.Lippold, et al, Automatic Counting of Fission Tracks using Object-Based Image Analysis for Dating Applications: IEEE; 2007 .
- 20 HAN Zhong-zhi, et al, Counting Ear Rows in Maize Using Image Process Method, China: IEEE ; 2010.
- 21 Tim K.Lee, et al, Counting Moles Automatically From Back Images: IEEE Transaction on biomedical engineering; 2005: 52; 1966-1969.
- 22 Stanley C.Best, et al, Evaluation of spatial and temporal variability of the physical characteristics of berries olives (*Olea europaea* L.), Arbequina variety,using image technology processing, Chile.
- 23 Geisa M.Faustino, et al, Automatic Embryonic Stem Cells Detection and Counting Method in Fluorescence Microscopy Images, Brazil: IEEE; 2009.
- 24 Emmanuel Kondela, Huang Dong Jun, "A Power Law Transformation Predicting Lightness Conditions Based on Skin Color Space Detection"; International Joint Conference of IEEE; 2011.
- 25 Allin Cottrell , "Regression Analysis: Basic Concepts", 2011.

APPENDICES

APPENDIX A

THE RELATIONSHIP BETWEEN THE OPTIMAL THRESHOLD AND GAMMA CORRECTION OF P.ACNE IMAGE BY SAMPLE REGRESSION ANALYSIS USING SPSS Tool

1. Regression

Variables Entered/Removed^a

Model	Variables Entered	Variables Removed	Method
1	Low-input threshold ^b	.	Enter

a. Dependent Variable: Optimal threshold

b. All requested variables entered.

Model Summary^b

Model	R	R Square	Adjusted R Square	Std. Error of the Estimate	Durbin-Watson
1	.990 ^a	.981	.980	.00424	1.874

a. Predictors: (Constant), Low-input threshold

b. Dependent Variable: Optimal threshold

ANOVA^a

Model	Sum of Squares	df	Mean Square	F	Sig.
Regression	.044	1	.044	2421.301	.000 ^b
Residual	.001	48	.000		
Total	.044	49			

a. Dependent Variable: Optimal threshold

b. Predictors: (Constant), Low-input threshold

Coefficients^a

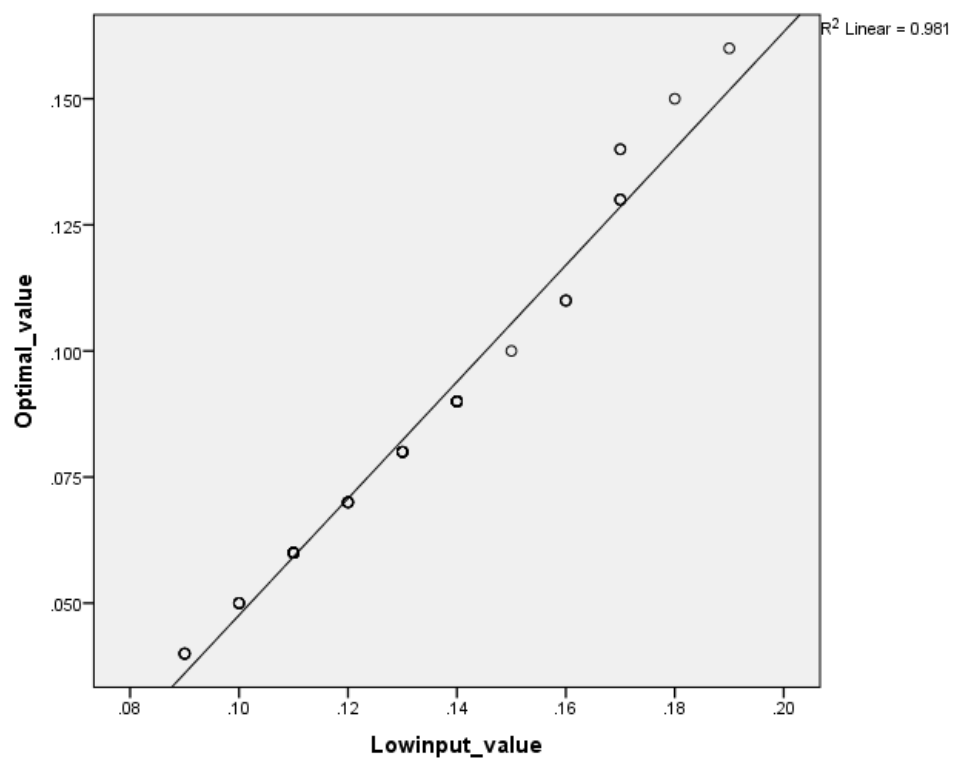
Model	Unstandardized Coefficients		Standardized Coefficients	t	Sig.	95.0% Confidence Interval for B	
	B	Std. Error	Beta			Lower Bound	Upper Bound
(Constant)	-.068	.003		21.969	.000	-.074	-.062
Low-input threshold	1.156	.023	.990	49.207	.000	1.109	1.203

a. Dependent Variable: Optimal threshold

Residuals Statistics^a

	Minimum	Maximum	Mean	Std. Deviation	N
Predicted Value	.0361	.1517	.0814	.02981	50
Residual	-.00701	.01143	.00000	.00420	50
Std. Predicted Value	-1.521	2.358	.000	1.000	50
Std. Residual	-1.654	2.694	.000	.990	50

a. Dependent Variable: Optimal threshold



2. Descriptive

Descriptive Statistics

	N	Minimum	Maximum	Mean	Std. Deviation
Optimal threshold	50	.04	.16	.0814	.03010
Low-input threshold	50	.09	.19	.1292	.02578
Valid N (listwise)	50				

3. Frequencies

Statistics

	Image No	th1	th2	th3	Optimal threshold	Low-input threshold
N Valid	50	50	50	50	50	50
Missing	0	0	0	0	0	0
Std. Error of Mean		.0040178	.0038318	.0026119	.00426	.00365
Std. Deviation		.0284104	.0270947	.0184687	.03010	.02578
Variance		.001	.001	.000	.001	.001
Skewness		1.304	1.151	2.023	.875	.479
Std. Error of Skewness		.337	.337	.337	.337	.337
Kurtosis		1.573	1.025	5.720	.196	-.533
Std. Error of Kurtosis		.662	.662	.662	.662	.662
Range		.1255	.1137	.1020	.12	.10
Minimum		.0392	.0353	.0078	.04	.09
Maximum		.1647	.1490	.1098	.16	.19

4. Correlations

Descriptive Statistics

	Mean	Std. Deviation	N
Optimal threshold	.0814	.03010	50
Low-input threshold	.1292	.02578	50

Correlations

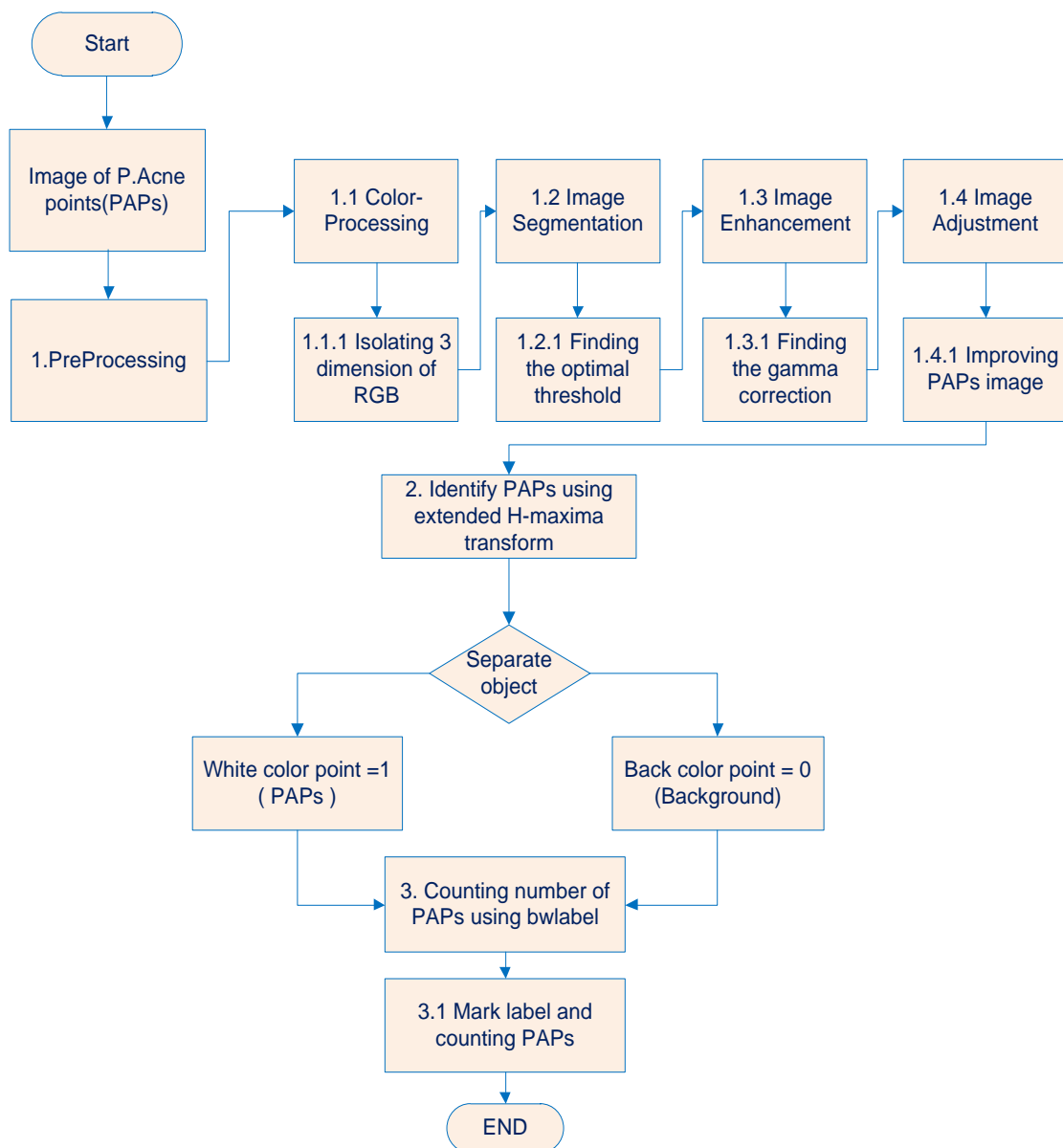
		Optimal threshold	Low-input threshold
Optimal threshold	Pearson Correlation	1	.990**
	Sig. (2-tailed)		.000
	Sum of Squares and Cross-products	.044	.038
	Covariance	.001	.001
	N	50	50
Low-input threshold	Pearson Correlation	.990**	1
	Sig. (2-tailed)	.000	
	Sum of Squares and Cross-products	.038	.033
	Covariance	.001	.001
	N	50	50

** . Correlation is significant at the 0.01 level (2-tailed).

APPENDIX B

FLOW CHART OF COUNTING P.ACNE POINTS BY THE IMAGE PROCESSING

1. Flow chart of the image processing

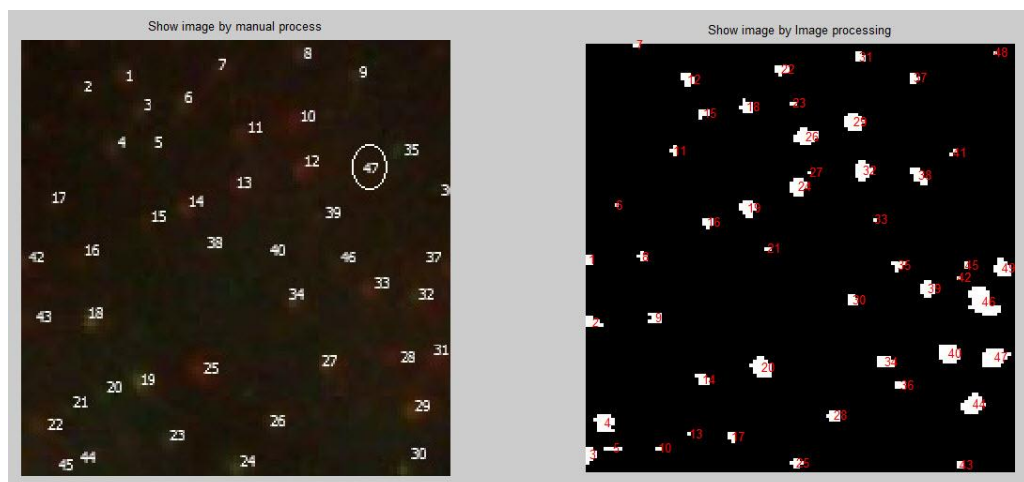


APPENDIX C

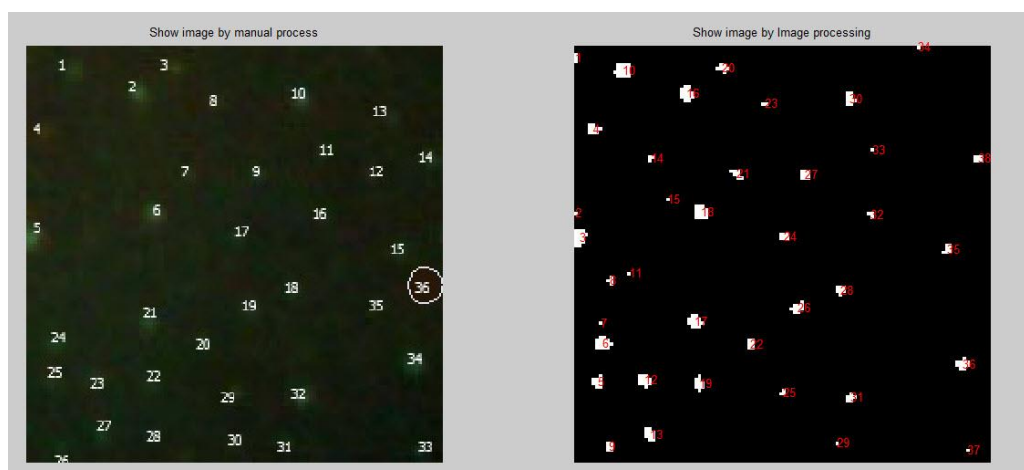
COMPARING THE P.ACNE IMAGE BETWEEN THE MANUAL COUNTING AND THE IMAGE PROCESSING

1. Demonstration of comparing objects

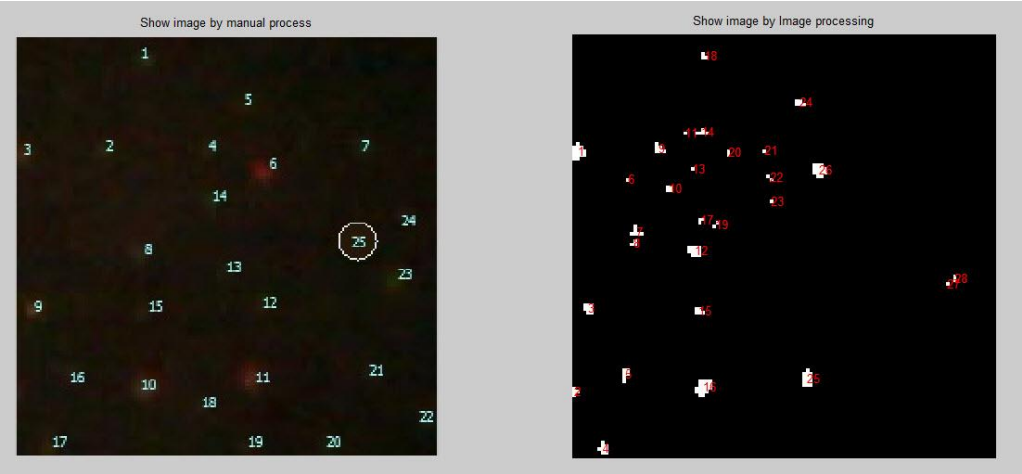
Sample image Data1



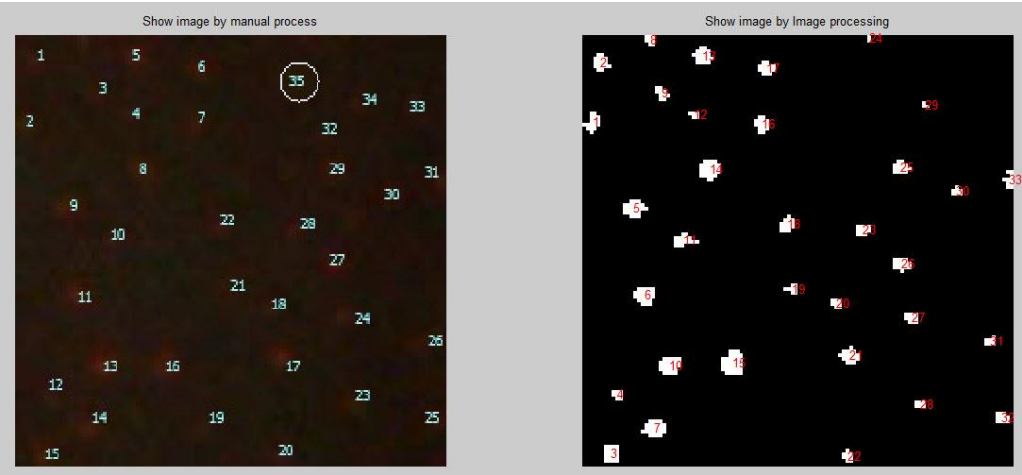
Sample image Data2



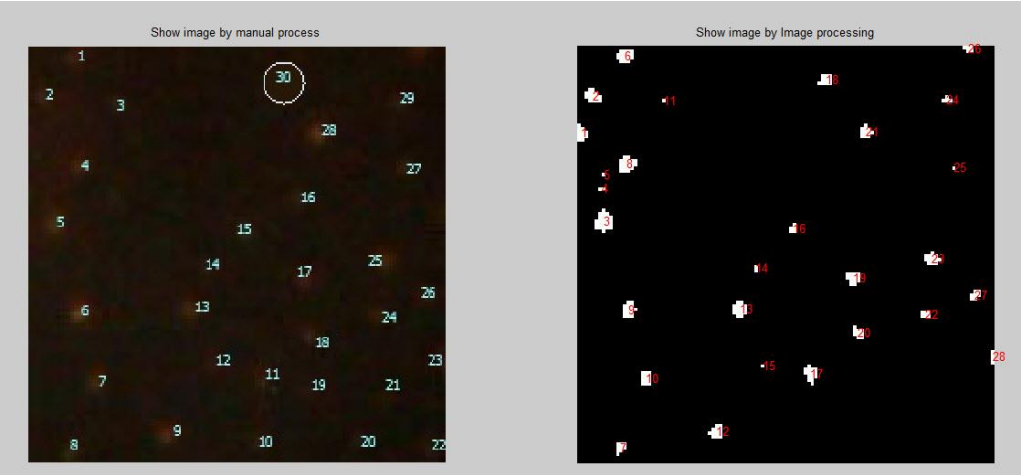
Sample image Data3



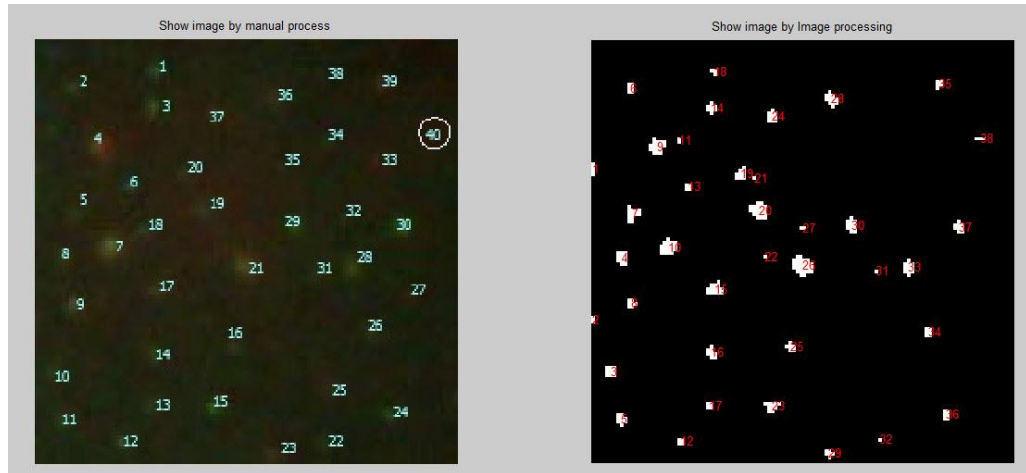
Sample image Data4



Sample image Data5



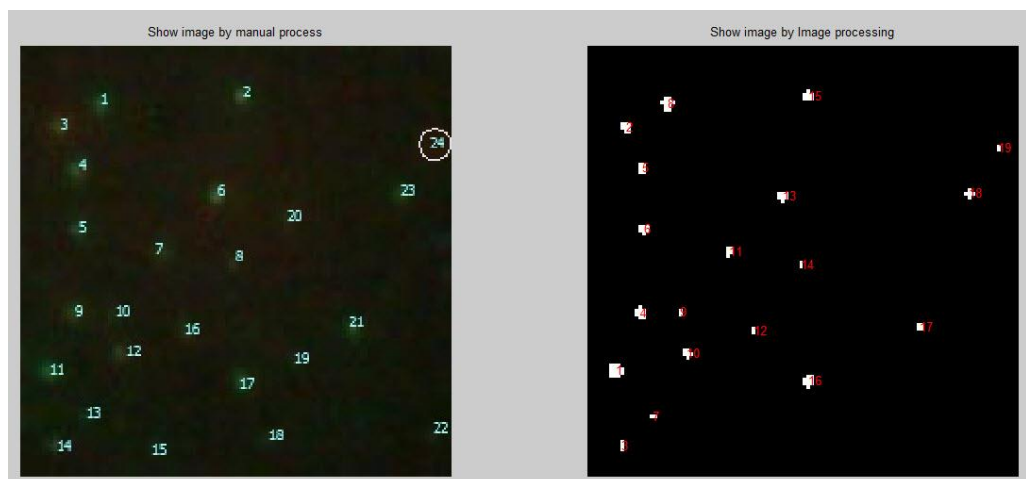
Sample image Data6



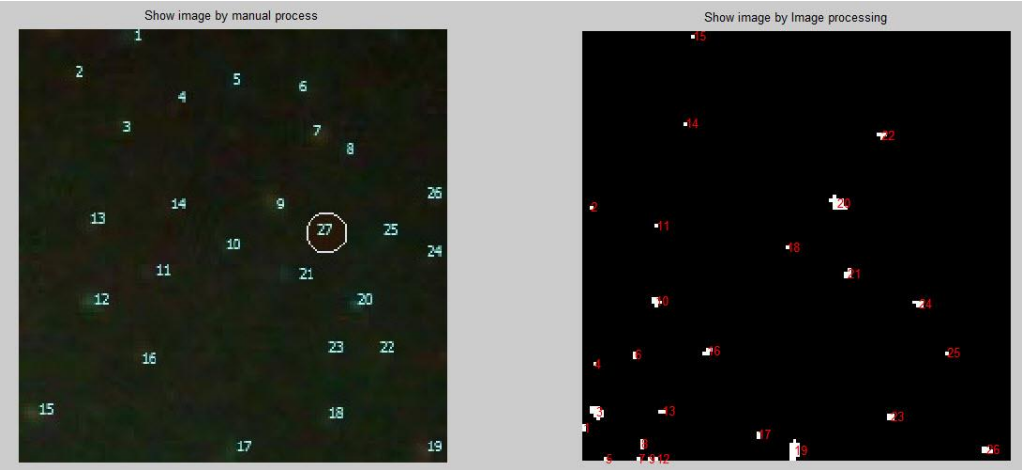
Sample image Data7



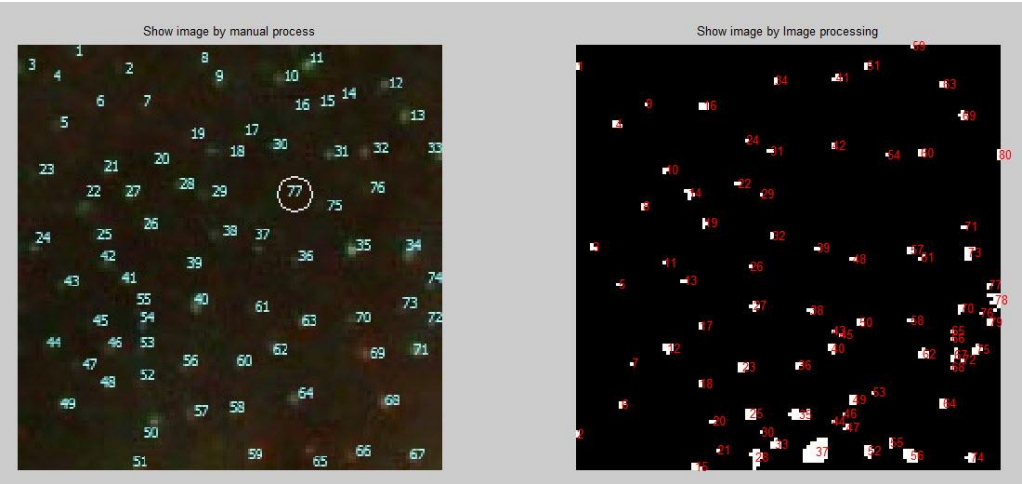
Sample image Data8



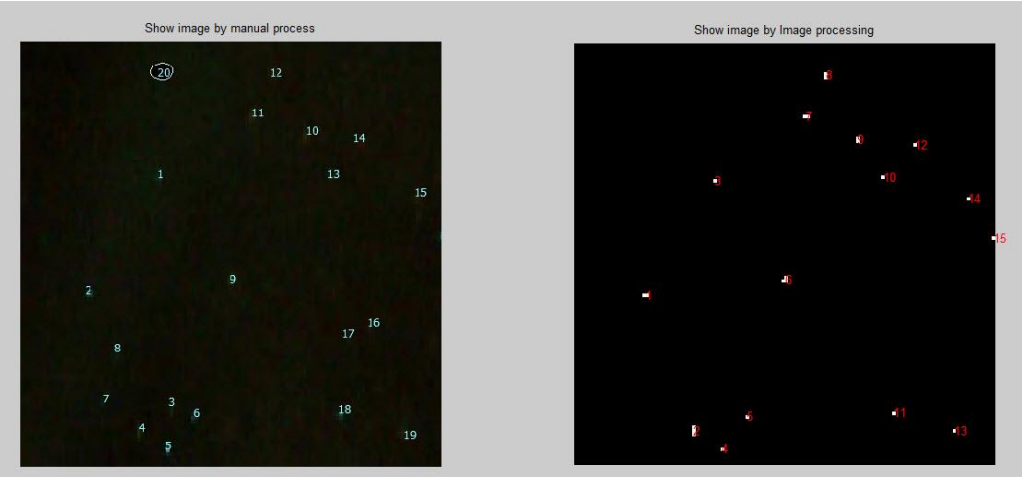
Sample image Data9



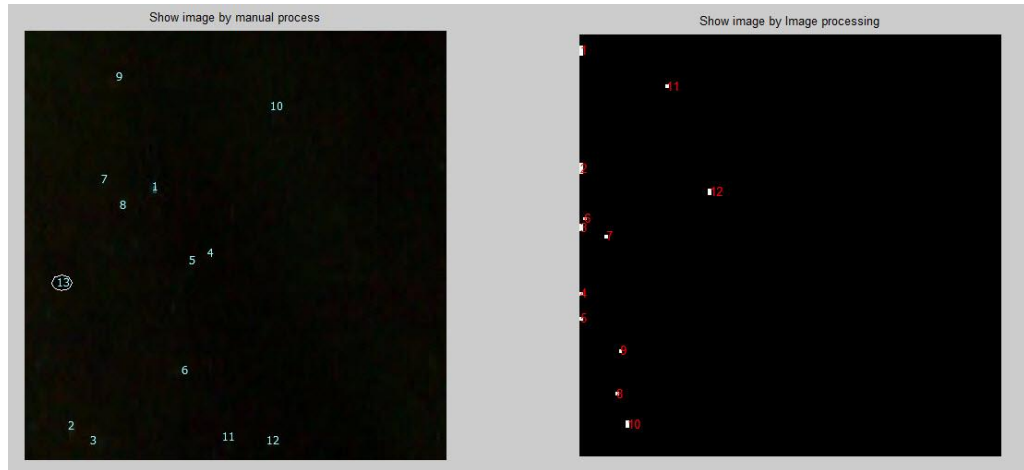
Sample image Data10



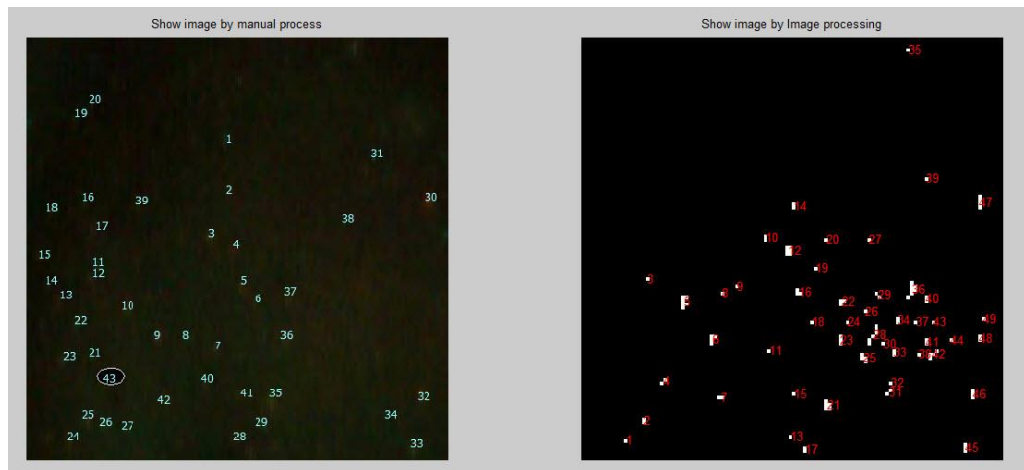
Sample image Data11



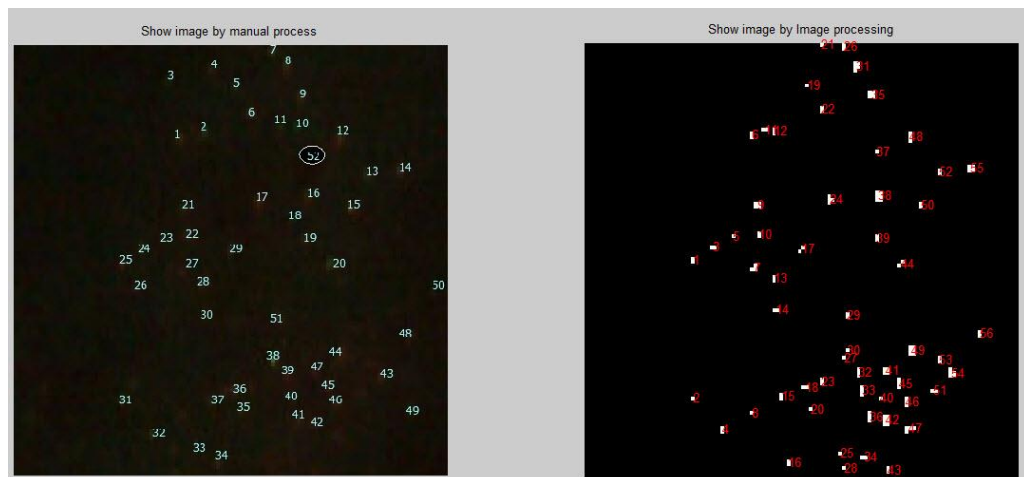
Sample image Data12



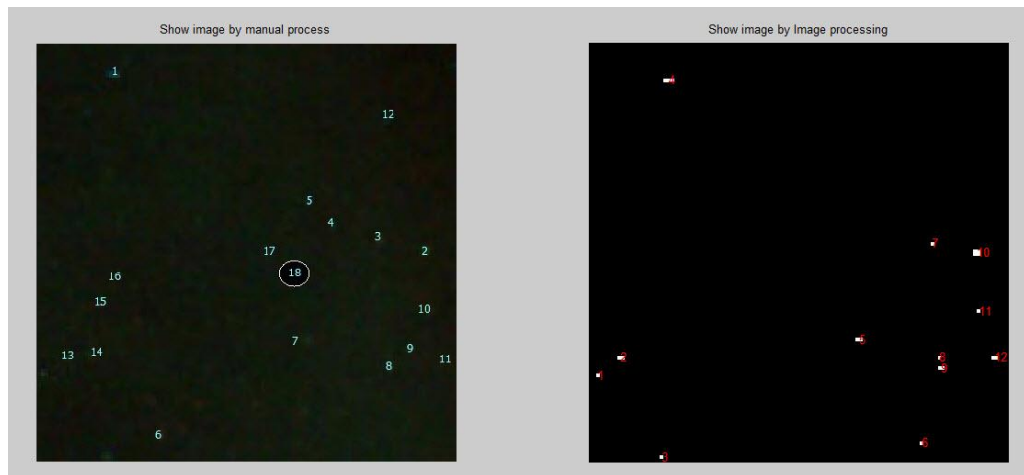
Sample image Data13



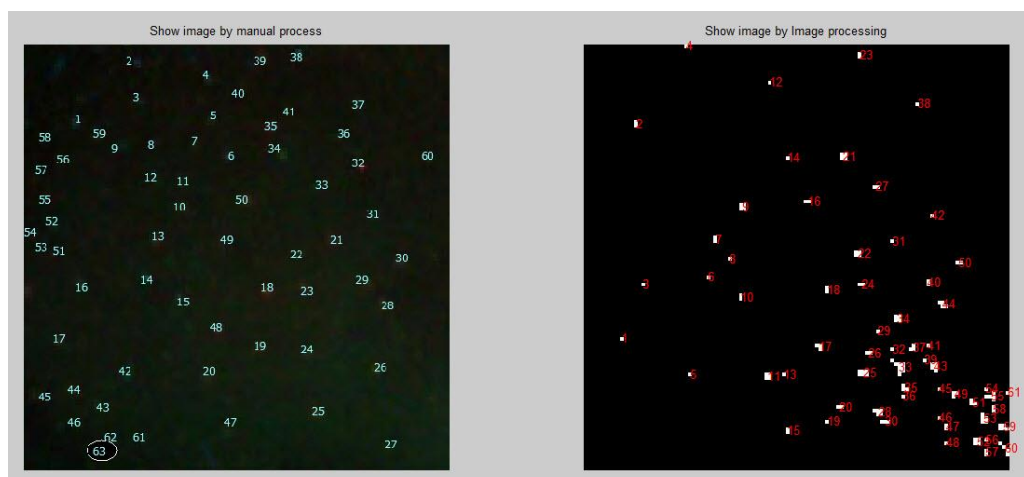
Sample image Data14



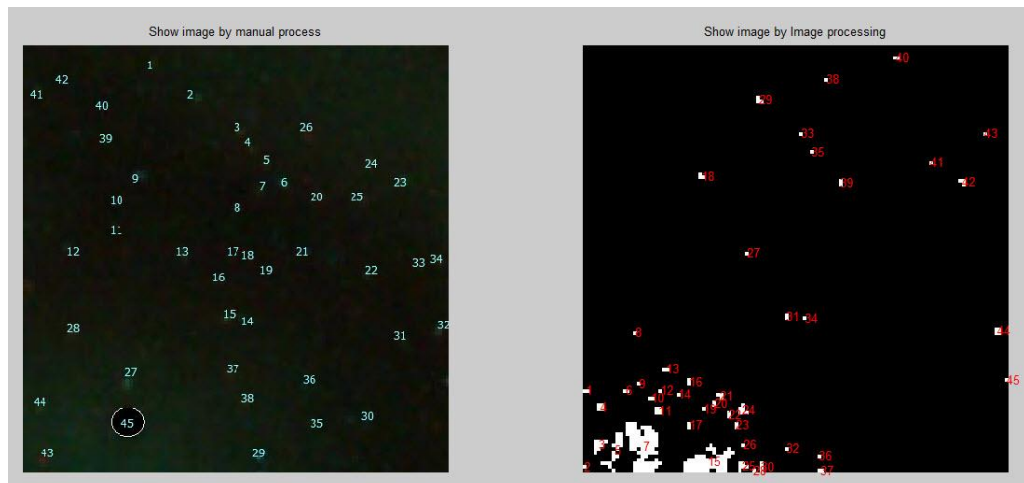
Sample image Data15



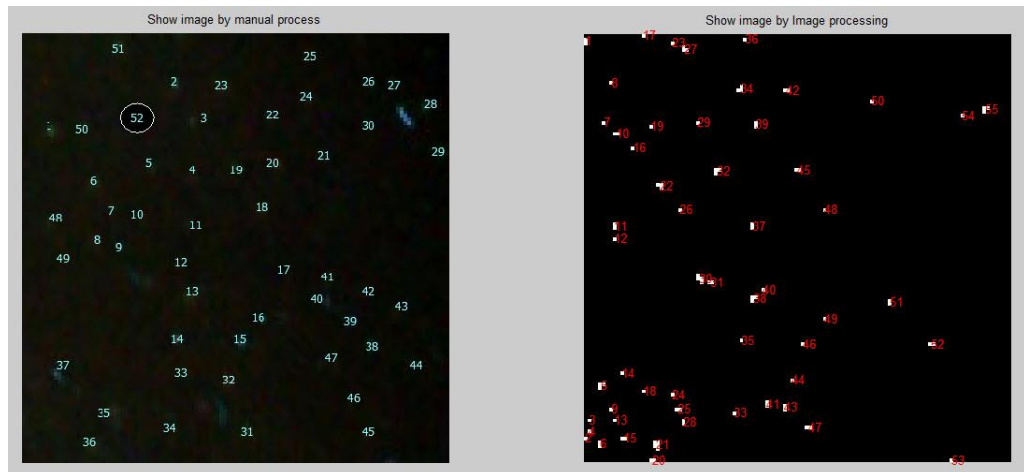
Sample image Data16



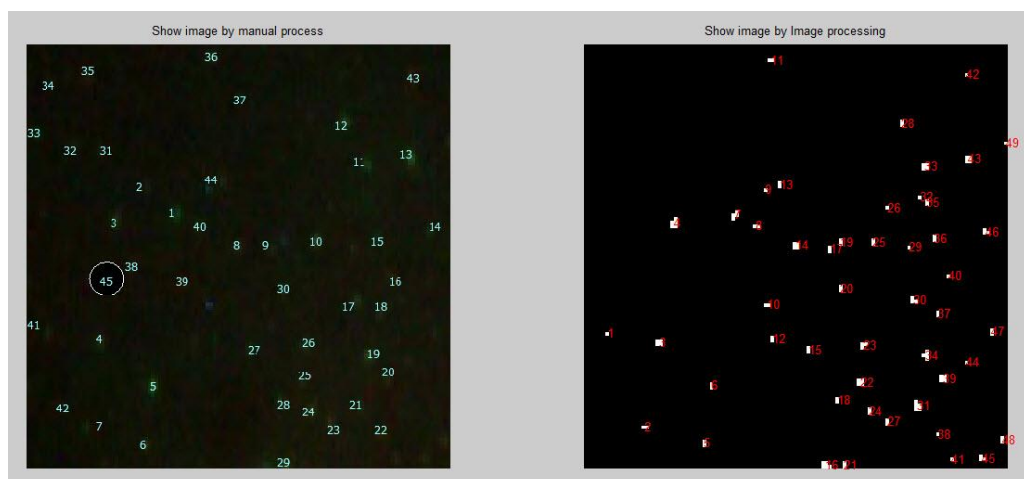
Sample image Data17



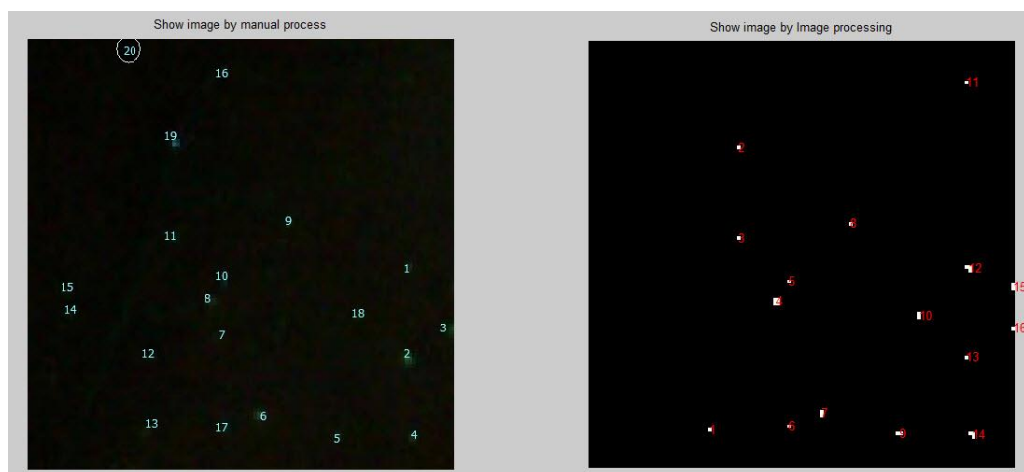
Sample image Data18



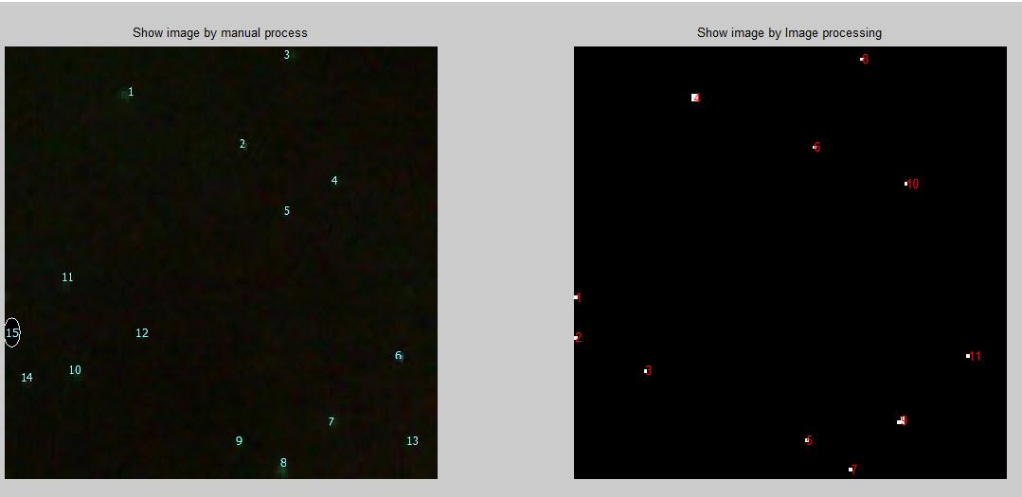
Sample image Data19



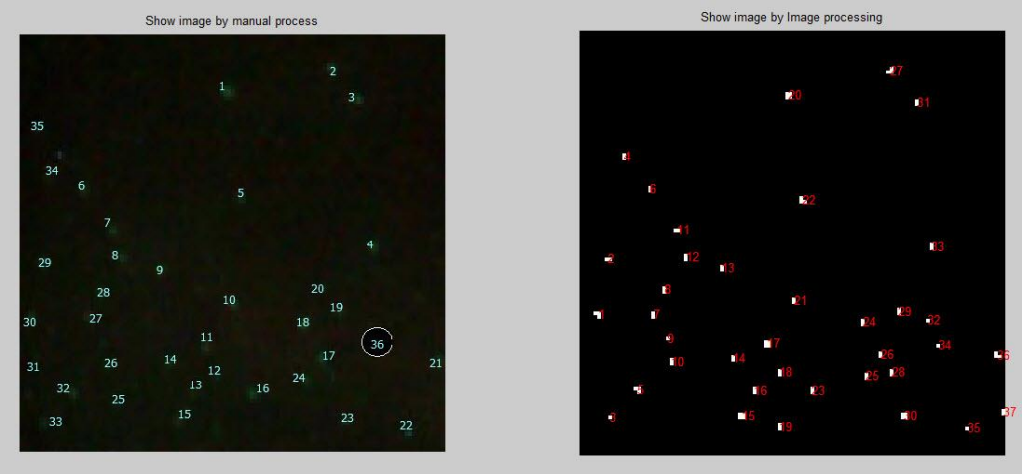
Sample image Data20



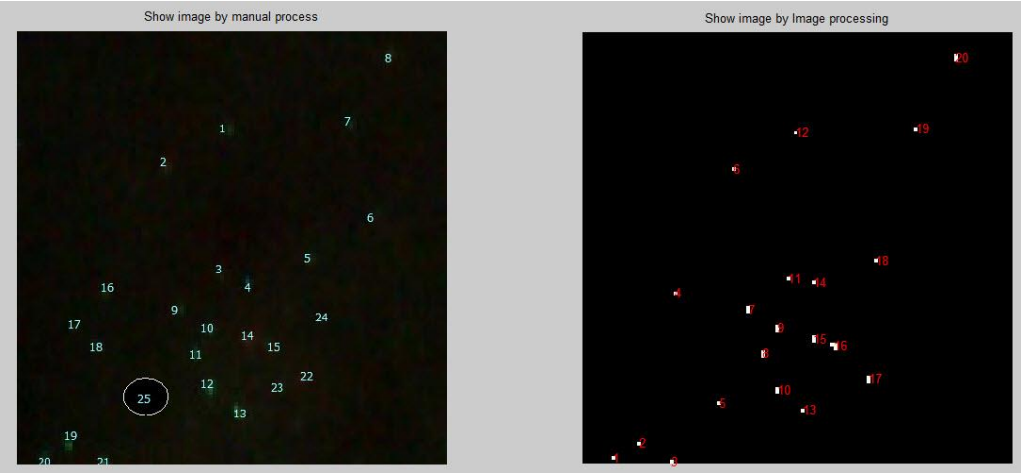
Sample image Data21



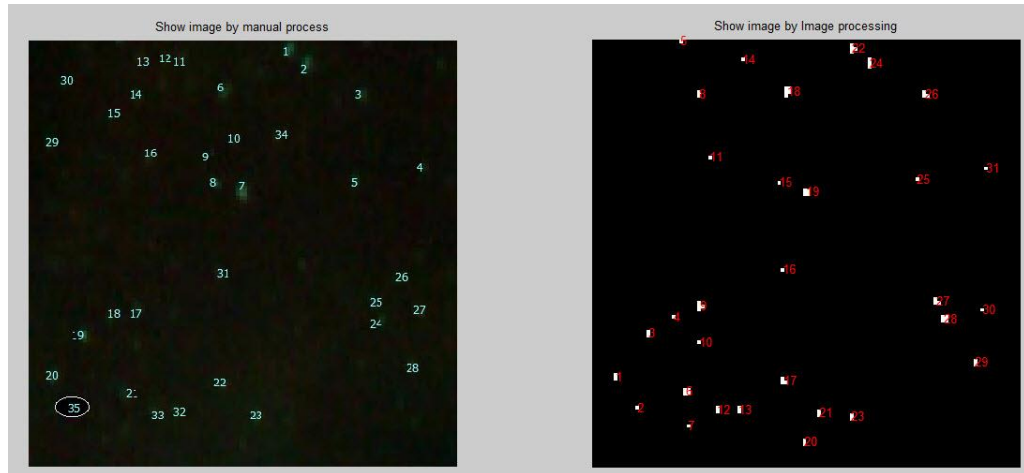
Sample image Data22



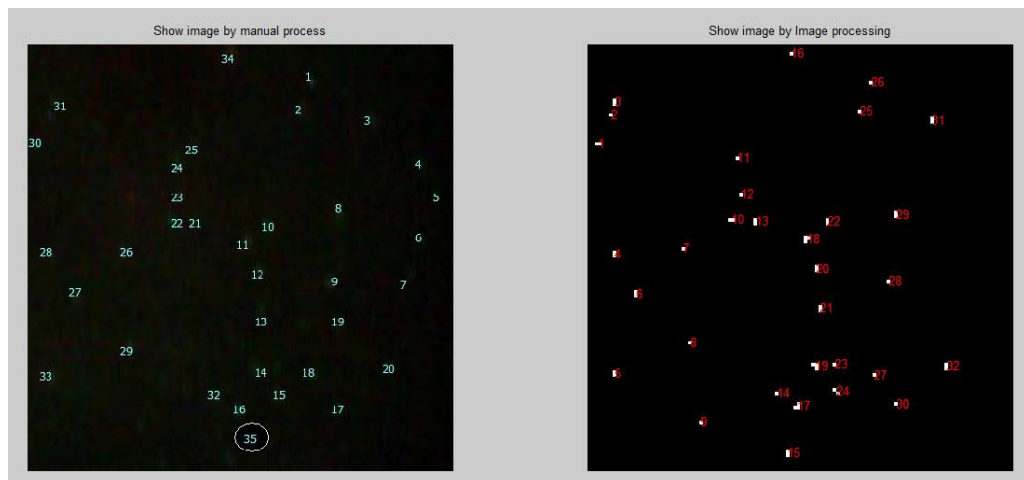
Sample image Data23



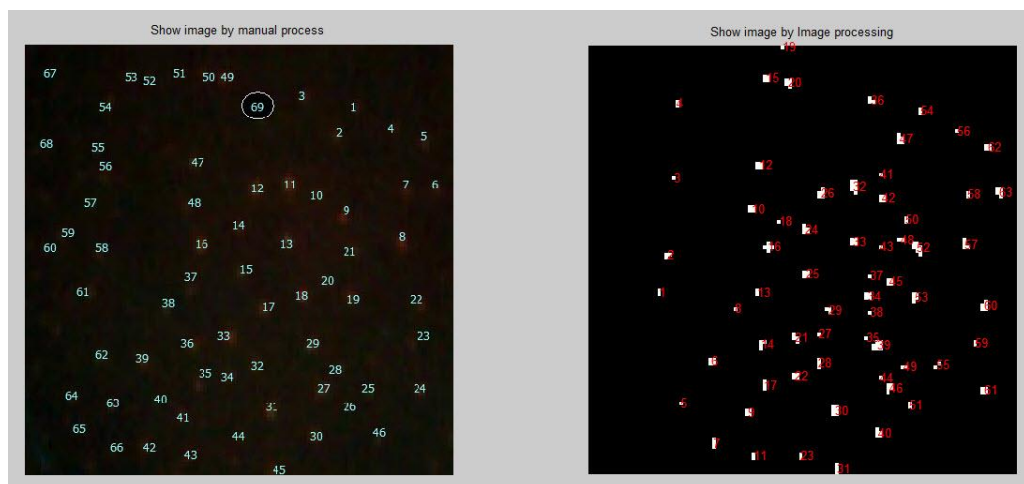
Sample image Data24



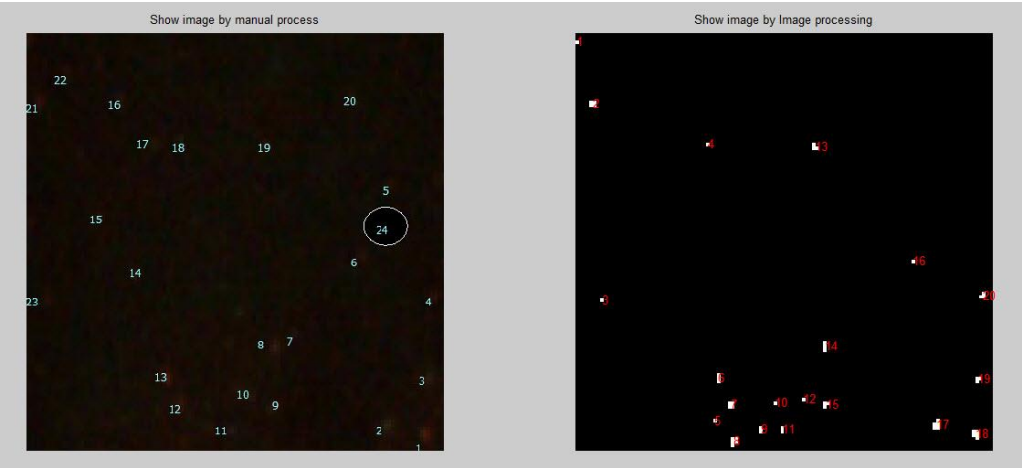
Sample image Data25



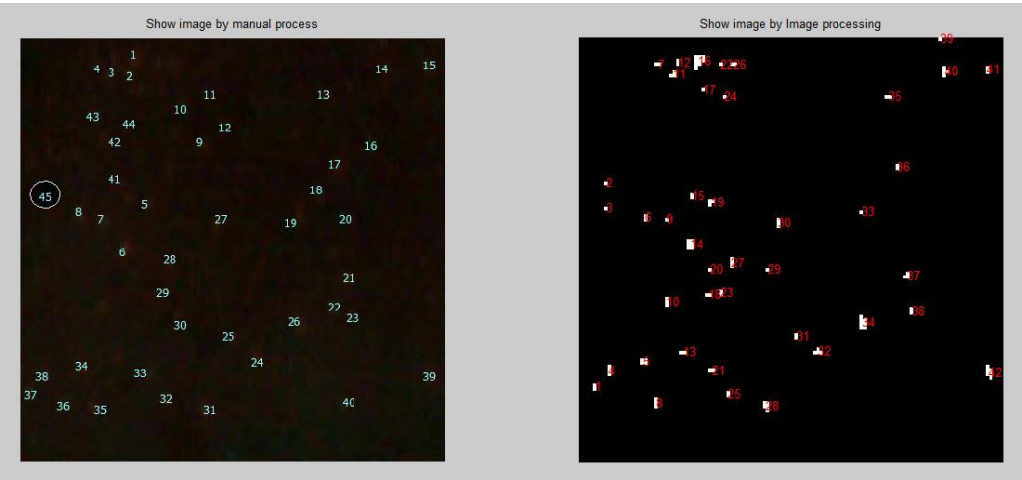
Sample image Data26



Sample image Data27



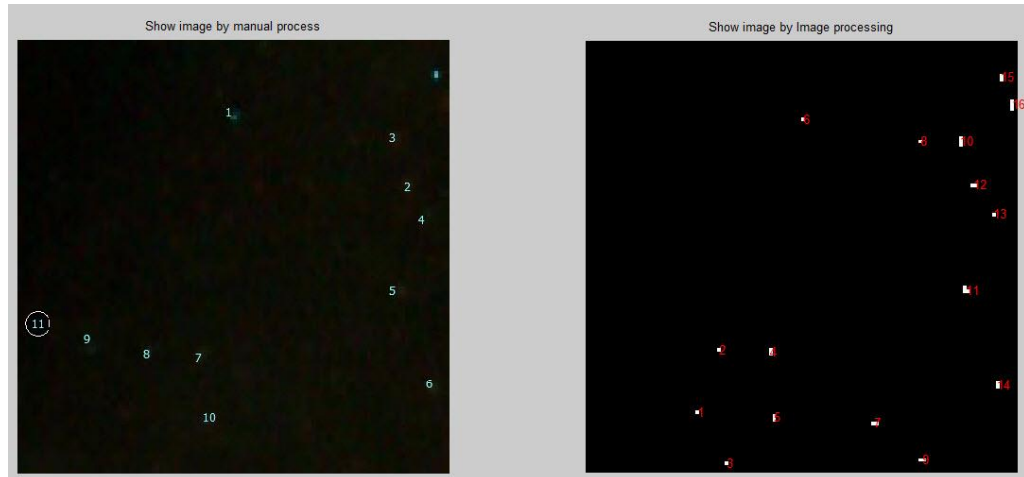
Sample image Data28



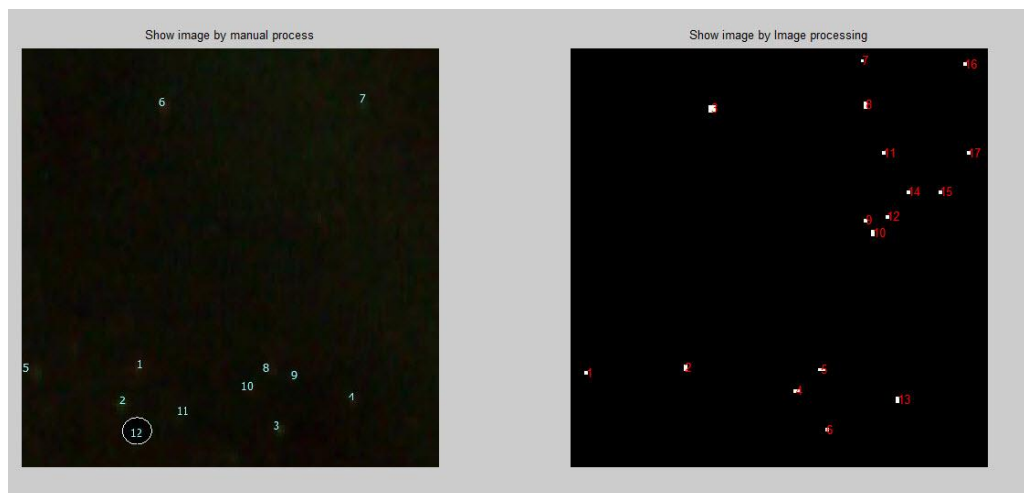
Sample image Data29



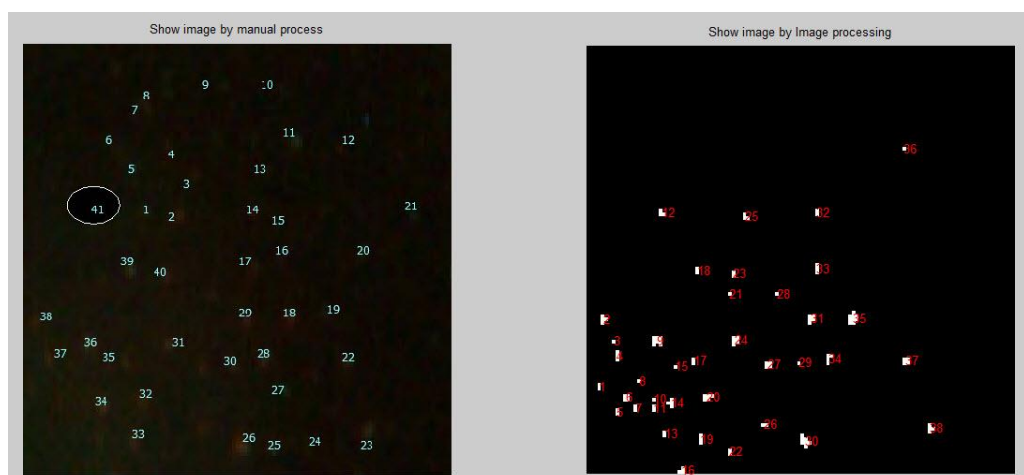
Sample image Data30



Sample image Data31



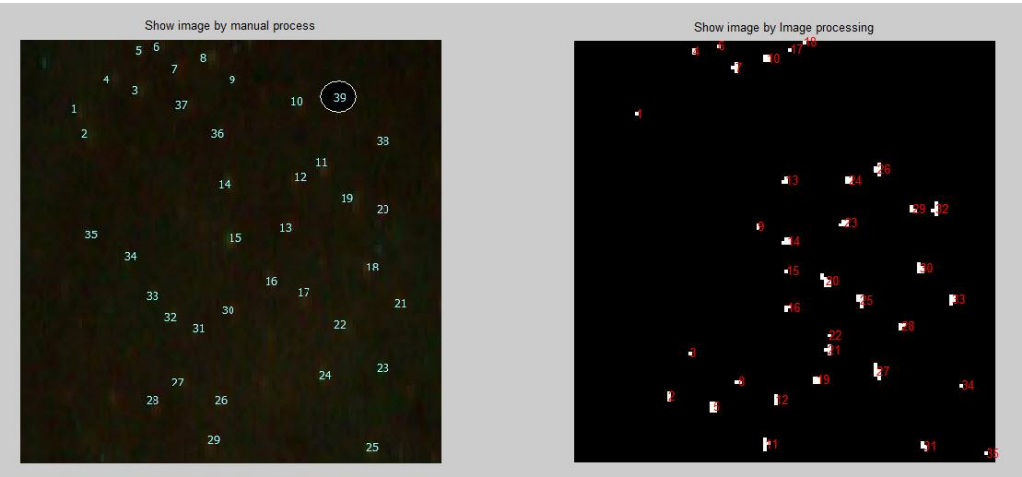
Sample image Data32



Sample image Data33



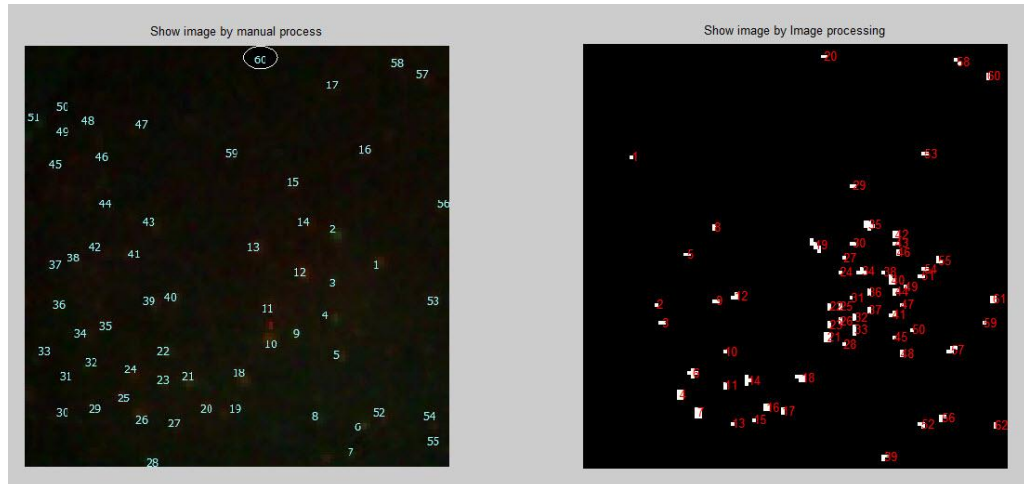
Sample image Data34



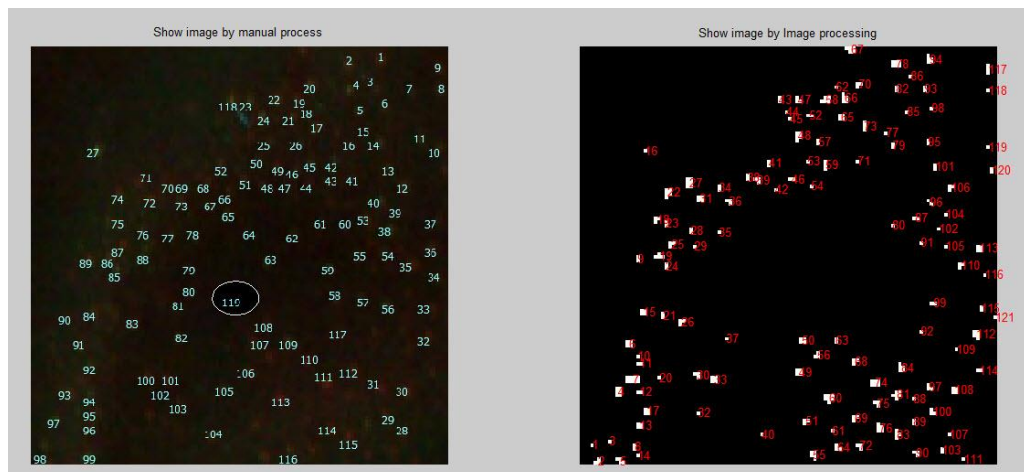
Sample image Data35



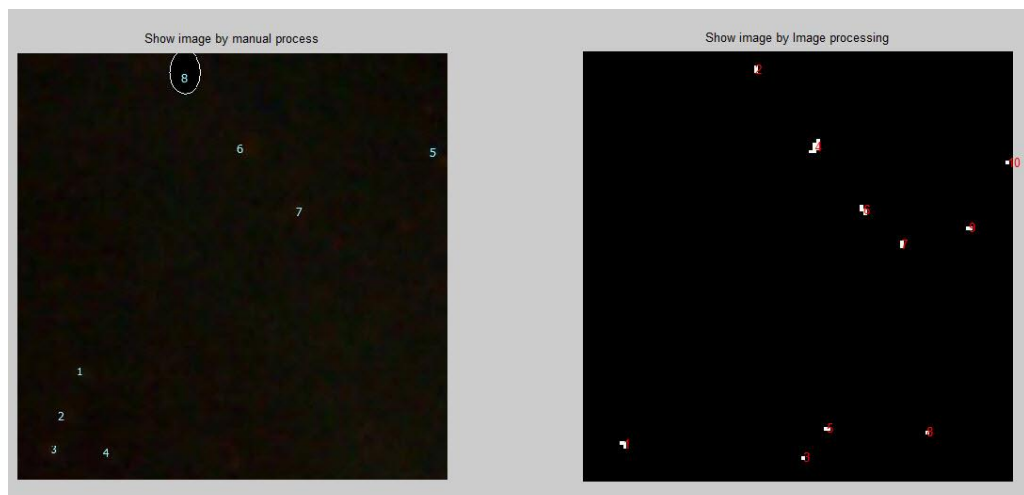
Sample image Data36



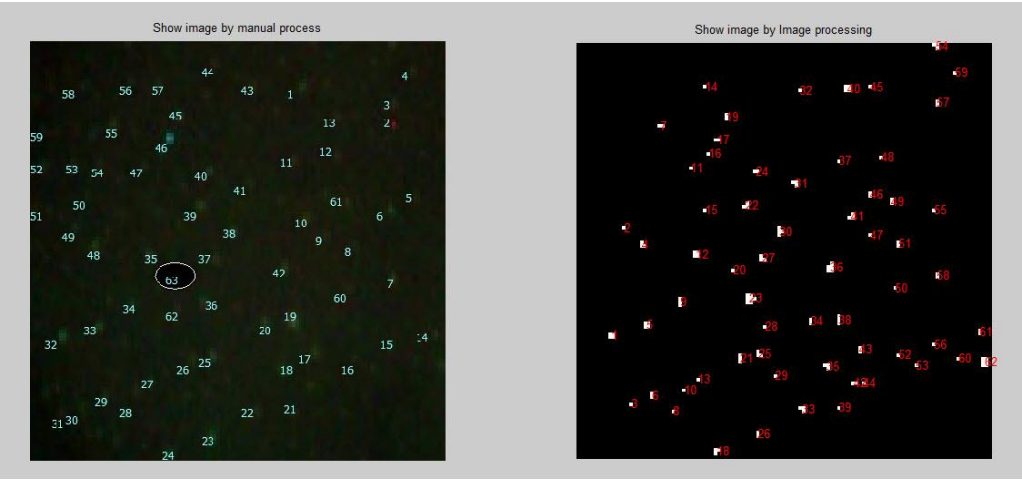
Sample image Data37



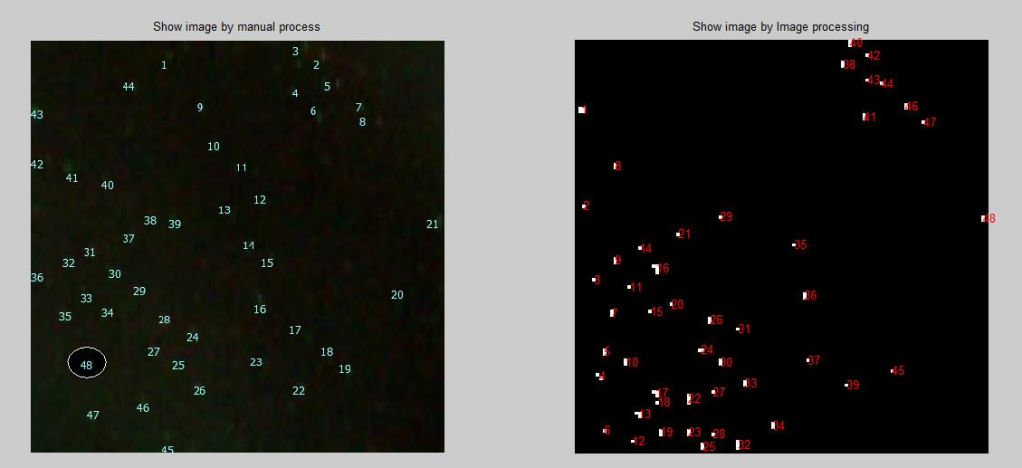
Sample image Data38



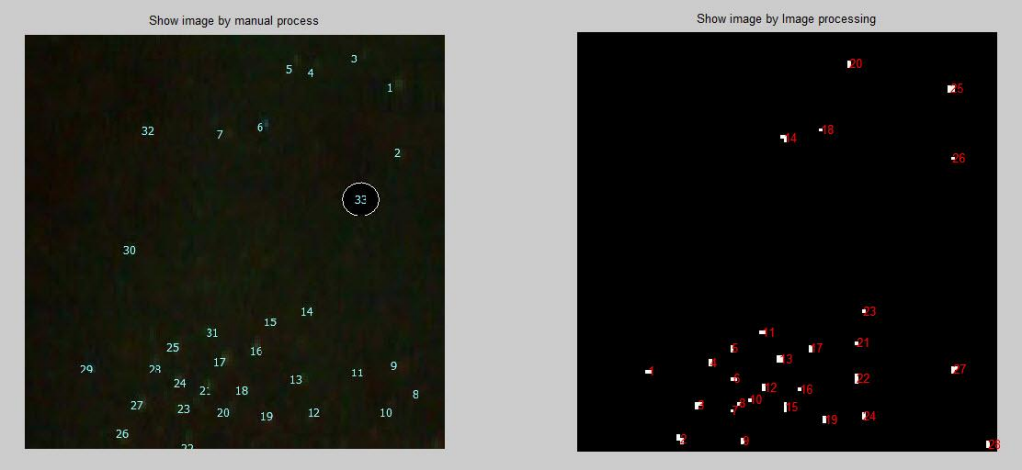
Sample image Data39



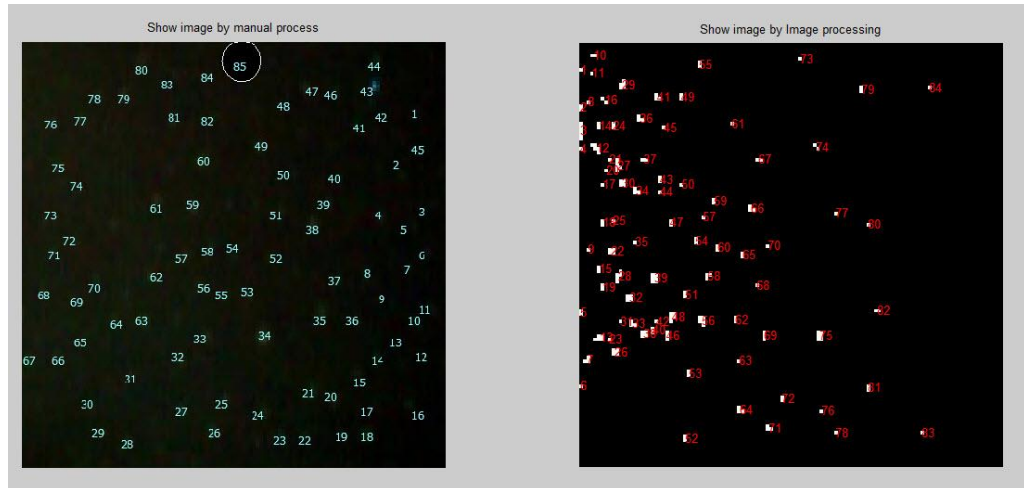
Sample image Data40



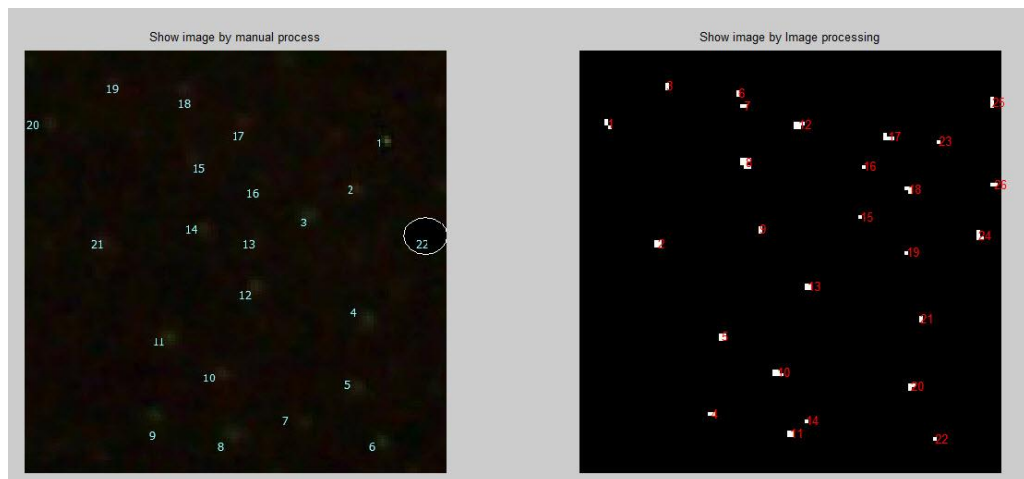
Sample image Data41



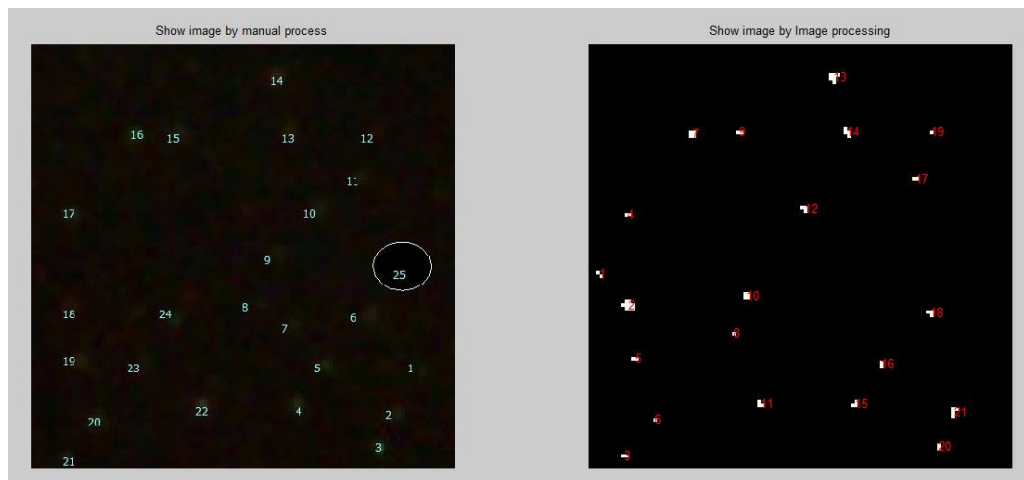
Sample image Data42



Sample image Data43



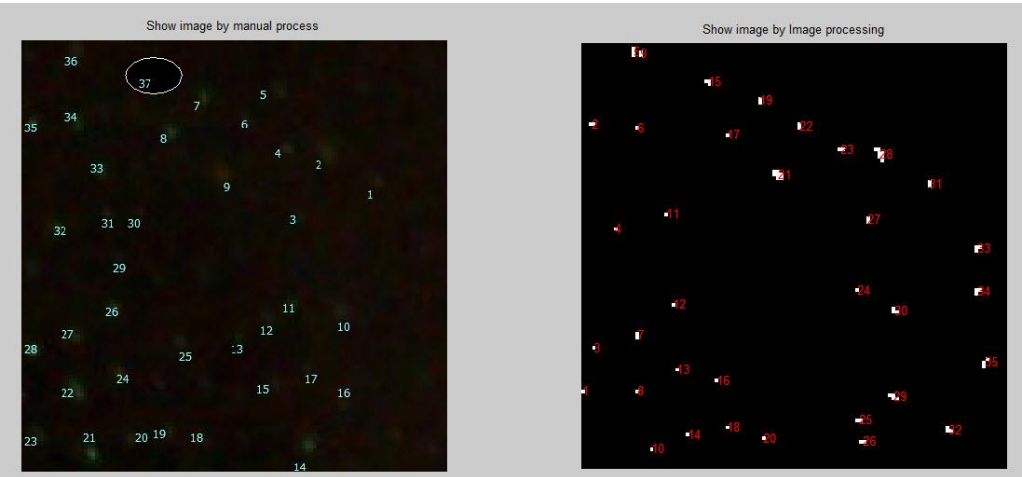
Sample image Data44



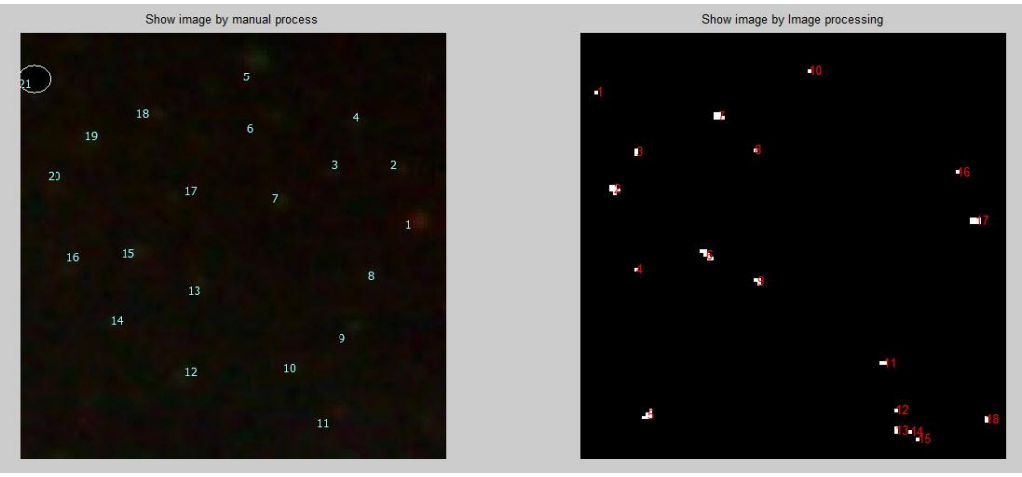
Sample image Data45



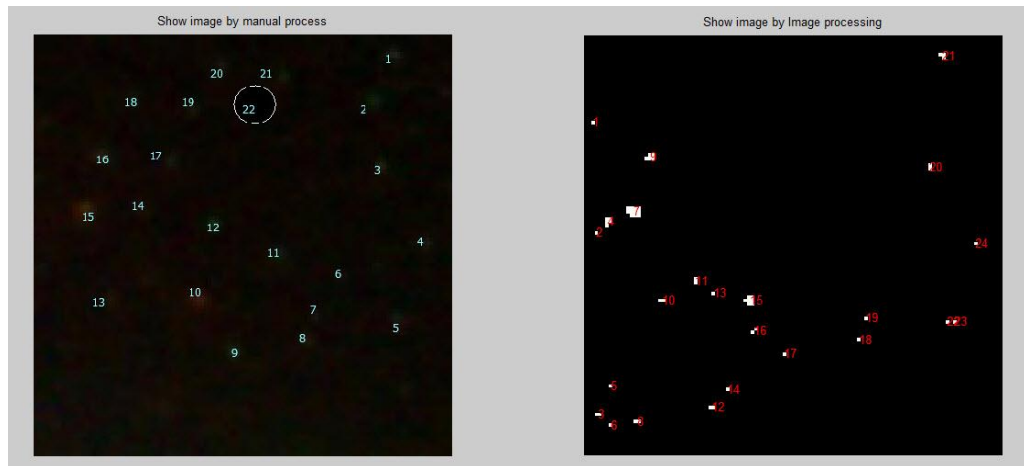
Sample image Data46



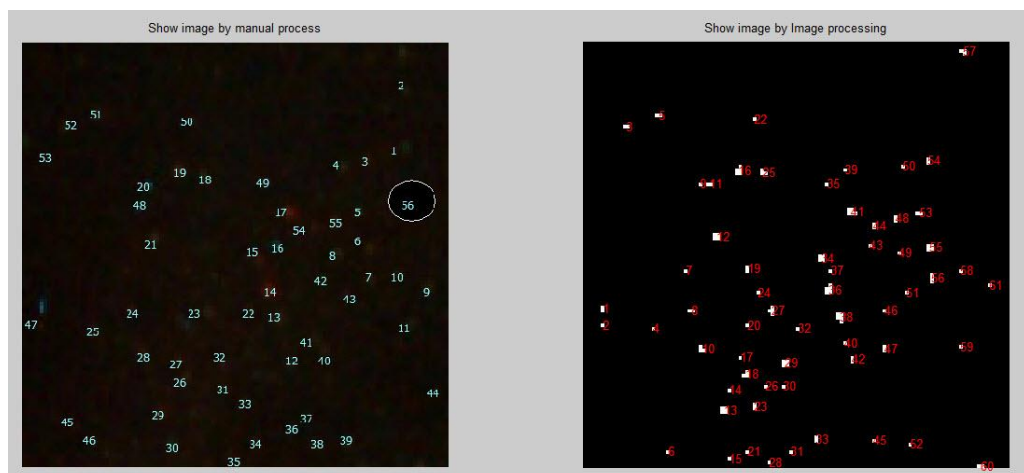
Sample image Data47



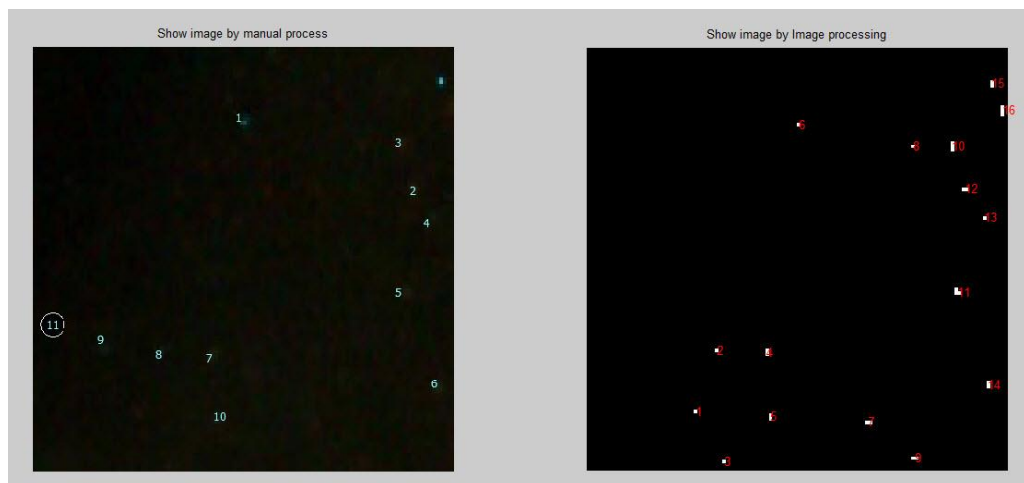
Sample image Data48



Sample image Data49



Sample image Data50



2. Image processing coding in MATLAB program

```

clear all
close all
clc

%%%%%%%%Input image%%%%%%%%

I = imread('img0027-4.jpg'); %% input P.Acne image
O = imread('img0027-4_c.jpg');
[s1,s2] = size(I)

%%%%%%%%Show RGB Layer From region image%%%%%%%%
figure,
subplot(2,2,1), imshow(I),title('Original image') %Original
subplot(2,2,2), imshow(I(:,:,1)),title('Red color') %R
subplot(2,2,3), imshow(I(:,:,2)),title('Green color') %G
subplot(2,2,4), imshow(I(:,:,3)),title('Blue color') %B

%%%Select Layer of image%%%%%%%%%%%%
th1= graythresh(I(:,:,1))
th2= graythresh(I(:,:,2))
th3= graythresh(I(:,:,3))

%%%%%%%%Find max value of threshold From RGB Layer in image%%%%%%%%
if(th1 > th2)&(th1 > th3)
    th_max = th1
    ia = I(:,:,1);
elseif (th2 > th1)&&(th2 > th3)
    th_max = th2
    ia = I(:,:,2);
elseif (th3 > th1)&&(th3 > th2)
    th_max = th3
    ia = I(:,:,3);
elseif (th1==th2)
    th_max = th1
    ia = I(:,:,1);
end

%%%Find gamma level threshold from max threshold of RGB image%%%

th_check = roundn(th_max, -2)

if(th_check>=0.17)
    low_in = 0.20;
elseif(th_check >= 0.16)

```

```

    low_in = 0.19;
    elseif(th_check >= 0.15)
    low_in = 0.18;
    elseif(th_check >= 0.12)
    low_in = 0.17;
    elseif(th_check >= 0.11)
    low_in = 0.16;
    elseif(th_check >= 0.10)
    low_in = 0.15;
    elseif(th_check >= 0.09)
    low_in = 0.14;
    elseif(th_check >= 0.08)
    low_in = 0.13;
    elseif(th_check >= 0.07)
    low_in = 0.12;
    elseif(th_check >= 0.06)
    low_in = 0.11;
    elseif(th_check >= 0.05)
    low_in = 0.10;
    elseif(th_check >= 0.04)
    low_in = 0.09;
end
low_input = low_in

%%%%%%%%%%%% Image Enhancement for adjustment image%%%%%%%%
% low_out = 1;
% high_out = 0;
% gamma = 0.3;
% high_in = 0.8;
% low_in = low_input;
%J = imadjust(ia,[low_in high_in],[low_out high_out],gamma);
ia2= imadjust(ia,[low_input 0.8],[0 1],0.3)
figure,
subplot(2,2,1), imshow(ia),title('Image before adjustment') %not adjust
subplot(2,2,2), imhist(ia),title('the histogram before adjustment') %not adjust
subplot(2,2,3), imshow(ia2),title('Image after adjustment add gamma') %not adjust
subplot(2,2,4), imhist(ia2),title('the histogram after adjustment') %not adjust
%%%%%%%%%%%% Image Segmentation of image%%%%%%%%
%%BW = imextendedmax(I,H) computes the extended-maxima transform, which is
the regional maxima of the H-maxima transform. H is a nonnegative scalar
%%Regional maxima are connected components of pixels with a constant intensity
value, and whose external boundary pixels all have a lower value.
% BW = IMEXTENDEDMAX(I,H,CONN) computes the extended maxima
transform,
% where CONN specifies the connectivity. CONN may have the following
% scalar values:
%
% 4 two-dimensional four-connected neighborhood

```

```

%      8    two-dimensional eight-connected neighborhood
%      6    three-dimensional six-connected neighborhood
%     18    three-dimensional 18-connected neighborhood
%     26    three-dimensional 26-connected neighborhood

bw = imextendedmax(ia2, th_check*255);
figure,
subplot(1,2,1), imshow(bw),title('Image segmentation by extended maxima
transfrom') %not adjust
subplot(1,2,2), imhist(bw),title('The histogram of Image segmentation by extended
maxima transfrom') %not adjust

%%%%%%%%%%Counting Number%%%%%%%%%%
[L2,n] = bwlabel(bw);
figure,
subplot(1,3,1),imshow(O),title('Show image by manual process')
subplot(1,3,2),imshow(I),title('Show Original image')
subplot(1,3,3),imshow(bw),title('Show image by Image processing');
hold on
for i=1:n
    [r,c]=find(L2==i);
    text(mean(c),mean(r),num2str(i),'color','red');
end

countacne = n

%%%%%%%%%%END%%%%%%%%%%

```

BIOGRAPHY

NAME	Ms.Manita Khongsuwan
DATE OF BIRTH	21 October 1986
PLACE OF BIRTH	Chumpon, Thailand
INSTITUTIONS ATTENDED	King Mungkut University of Technology Thonburi, 1/2005-1/2009 Bachelor of Science (Computer Science) Mahidol University, 2011-2013 Master of Science (Technology of Information System Management)
HOME ADDRESS	5/21 Moo 1 Tumbon Heungjorakea Amphur Mueng, Nakronpathom 73000 Tel. 085-155-6177 E-mail: manita.kho@gmail.com
PUBLICATION / PRESENTATION	Manita Khongsuwan, Counting Number of Acne Valgaris using UV Fluorescence and Image processing, Biomedical Engineering International Conference (BMEiCON) - 2011, 29-31 January 2012, Kantary Resort Hill, Chiang Mai, Thailand